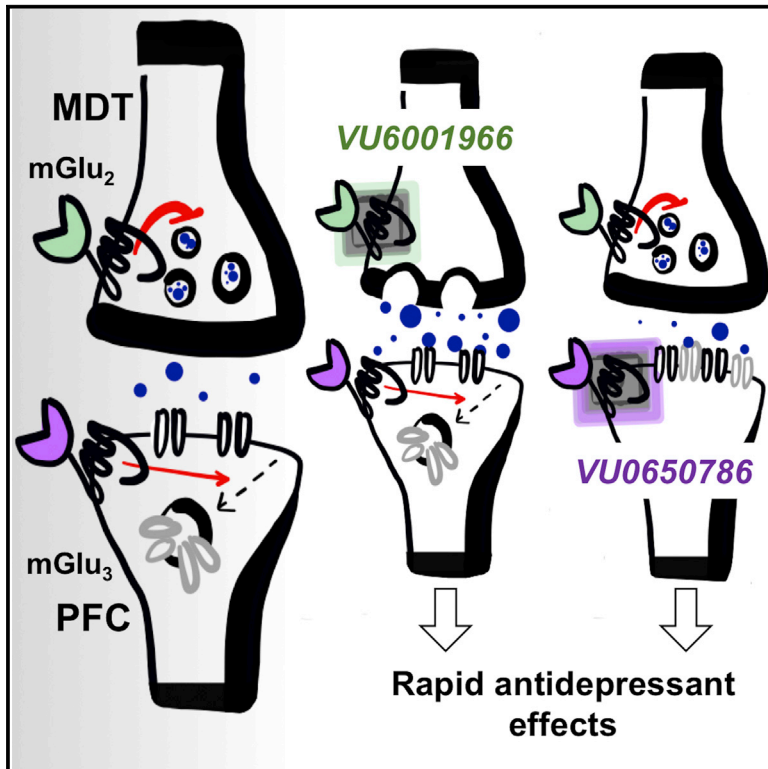


# Neuron

## mGlu<sub>2</sub> and mGlu<sub>3</sub> Negative Allosteric Modulators Divergently Enhance Thalamocortical Transmission and Exert Rapid Antidepressant-like Effects

### Graphical Abstract



### Authors

Max E. Joffe, Chiaki I. Santiago, Kendra H. Oliver, ..., Craig W. Lindsley, Danny G. Winder, P. Jeffrey Conn

### Correspondence

max.joffe@vanderbilt.edu (M.E.J.), jeff.conn@vanderbilt.edu (P.J.C.)

### In Brief

mGlu<sub>2/3</sub> antagonists exert antidepressant-like effects, but the requisite mechanisms remain unresolved. Joffe et al. leverage optimized negative allosteric modulators to interrogate the underlying neurocircuits, discovering that selective inhibition of either mGlu<sub>2</sub> or mGlu<sub>3</sub> enhances thalamocortical transmission and confers antidepressant-like efficacy across multiple models.

### Highlights

- mGlu<sub>2</sub> and mGlu<sub>3</sub> negative allosteric modulators (NAMs) stimulate prefrontal cortex
- mGlu<sub>2</sub> regulates thalamocortical glutamate release probability
- mGlu<sub>3</sub> directs prefrontal cortex postsynaptic plasticity
- mGlu<sub>2</sub> and mGlu<sub>3</sub> NAMs independently decrease passive coping and reverse anhedonia



# mGlu<sub>2</sub> and mGlu<sub>3</sub> Negative Allosteric Modulators Divergently Enhance Thalamocortical Transmission and Exert Rapid Antidepressant-like Effects

Max E. Joffe,<sup>1,2,3,7,\*</sup> Chiaki I. Santiago,<sup>2,4</sup> Kendra H. Oliver,<sup>1</sup> James Maksymetz,<sup>1,2</sup> Nicholas A. Harris,<sup>3,5</sup> Julie L. Engers,<sup>2</sup> Craig W. Lindsley,<sup>1,2,3,6</sup> Danny G. Winder,<sup>1,3,5</sup> and P. Jeffrey Conn<sup>1,2,3,8,\*</sup>

<sup>1</sup>Department of Pharmacology, Vanderbilt University, Nashville, TN 37232, USA

<sup>2</sup>Vanderbilt Center for Neuroscience Drug Discovery, Nashville, TN 37232, USA

<sup>3</sup>Vanderbilt Center for Addiction Research, Nashville, TN 37232, USA

<sup>4</sup>Vanderbilt University, Nashville, TN 37232, USA

<sup>5</sup>Department of Molecular Physiology and Biophysics, Vanderbilt University, Nashville, TN 37232, USA

<sup>6</sup>Department of Chemistry, Vanderbilt University, Nashville, TN 37232, USA

<sup>7</sup>Twitter: @mejoffe

<sup>8</sup>Lead Contact

\*Correspondence: [max.joffe@vanderbilt.edu](mailto:max.joffe@vanderbilt.edu) (M.E.J.), [jeff.conn@vanderbilt.edu](mailto:jeff.conn@vanderbilt.edu) (P.J.C.)

<https://doi.org/10.1016/j.neuron.2019.09.044>

## SUMMARY

Non-selective antagonists of metabotropic glutamate receptor subtypes 2 (mGlu<sub>2</sub>) and 3 (mGlu<sub>3</sub>) exert rapid antidepressant-like effects by enhancing prefrontal cortex (PFC) glutamate transmission; however, the receptor subtype contributions and underlying mechanisms remain unclear. Here, we leveraged newly developed negative allosteric modulators (NAMs), transgenic mice, and viral-assisted optogenetics to test the hypothesis that selective inhibition of mGlu<sub>2</sub> or mGlu<sub>3</sub> potentiates PFC excitatory transmission and confers antidepressant efficacy in preclinical models. We found that systemic treatment with an mGlu<sub>2</sub> or mGlu<sub>3</sub> NAM rapidly activated biophysically unique PFC pyramidal cell ensembles. Mechanistic studies revealed that mGlu<sub>2</sub> and mGlu<sub>3</sub> NAMs enhance thalamocortical transmission and inhibit long-term depression by mechanistically distinct presynaptic and postsynaptic actions. Consistent with these actions, systemic treatment with either NAM decreased passive coping and reversed anhedonia in two independent chronic stress models, suggesting that both mGlu<sub>2</sub> and mGlu<sub>3</sub> NAMs induce antidepressant-like effects through related but divergent mechanisms of action.

## INTRODUCTION

Conventional antidepressants fail to adequately treat more than two-thirds of patients with major depressive disorder (MDD) (Gaynes et al., 2009); thus, there is a tremendous unmet need to develop novel treatment approaches for affective disorders. Clinical studies have consistently revealed an association between MDD symptomology and prefrontal cortex (PFC) hypo-

function: MDD patients exhibit reduced total PFC volume (Caetano et al., 2006); impaired PFC activation during cognitive performance (Siegle et al., 2007); and reduced dendritic branching of pyramidal cells (Rajkowska, 2000). More specifically, reduced function of the glutamate system has been observed in the PFC of MDD patients (Hasler et al., 2007; Kang et al., 2012), especially in patients with symptoms within the research domain criteria positive valence systems, such as anhedonia (Walter et al., 2009). Conversely, pharmacological manipulations that enhance PFC glutamate transmission can exert robust antidepressant-like activity in animal models of anhedonia, as well as in behaviors modeling deficits in the negative valence systems, such as the forced swim test. Driving this research is the dissociative anesthetic ketamine, which increases excitatory transmission onto PFC pyramidal cells (Krystal et al., 2013) and acts as a rapid-acting antidepressant in treatment-resistant MDD patients and in rodent models (Kavalali and Monteggia, 2012; Zanos and Gould, 2018). Unfortunately, ketamine use is accompanied by several complications that limit its widespread clinical utility, but studies describing its efficacy and mechanism have prompted a major interest in exploring the potential of alternative means to enhance glutamate transmission in the PFC.

In recent years, the group II metabotropic glutamate (mGlu) receptor subtypes have emerged as exciting new targets for modulating excitatory transmission in the PFC (Gould et al., 2019; Joffe and Conn, 2019). The group II mGlu receptor family includes the mGlu<sub>2</sub> and mGlu<sub>3</sub> subtypes, which are classified together based on amino acid sequence homology, G-protein coupling, and pharmacology (Joffe et al., 2018). Within the PFC, expression of both mGlu<sub>2</sub> and mGlu<sub>3</sub> occurs at presynaptic terminals, and mGlu<sub>3</sub> is also highly expressed at postsynaptic locations and on glia (Jin et al., 2018; Ohishi et al., 1993b). Functionally, mGlu<sub>2/3</sub> activation suppresses spontaneous excitatory transmission (Bocchio et al., 2019; Kiritoshi and Neugebauer, 2015; Marek et al., 2000) and induces a robust, postsynaptic long-term depression (LTD) of evoked transmission in the PFC (Joffe et al., 2019a, 2019b). These studies raise the possibility that compounds that inhibit mGlu<sub>2</sub> and/or mGlu<sub>3</sub> could increase



synaptic excitation of the PFC by inhibiting presynaptic autoreceptors or reducing mGlu receptor-mediated LTD. Consistent with these actions, non-selective mGlu<sub>2/3</sub> antagonists, such as LY341495, are efficacious in preclinical models of antidepressant activity, decreasing immobility in the forced swim and tail suspension tests in both mice and rats (Chaki et al., 2004; Dong et al., 2017; Dwyer et al., 2013; Fukumoto et al., 2016). In etiologically relevant preclinical models of chronic stress, mGlu<sub>2/3</sub> antagonists rapidly reverse anhedonia (Dong et al., 2017; Dwyer et al., 2013) and prevent the induction of learned helplessness (Highland et al., 2019). Importantly, several studies have shown that stimulation of glutamate transmission in the PFC is necessary and sufficient for the antidepressant-like actions of mGlu<sub>2/3</sub> antagonists (Fukumoto et al., 2016; Highland et al., 2019), highlighting the impetus to interrogate PFC physiology to better understand the mechanisms mediating rapid antidepressant actions.

The antidepressant actions of mGlu<sub>2/3</sub> antagonists are often attributed to inhibition of mGlu<sub>2</sub> and therefore not mGlu<sub>3</sub>. Studies using knockout mice have revealed decreased passive coping behavior, learned helplessness, and stress-induced anhedonia following mGlu<sub>2</sub> genetic deletion (Highland et al., 2019; Morishima et al., 2005; Zanos et al., 2019). In addition, recent studies suggest that a major circulating metabolite of ketamine may exert antidepressant-relevant actions through a mechanism requiring reduced signaling by mGlu<sub>2</sub> receptors (Zanos et al., 2019). On the other hand, studies using mGlu<sub>3</sub> knockouts have been more limited and have delivered mixed findings with respect to passive coping (Highland et al., 2019; Morishima et al., 2005). Although these studies have provided important insight into the regulation of affective behaviors by mGlu receptors, innovating means to separately and rapidly modulate mGlu<sub>2</sub> and mGlu<sub>3</sub> in the adult CNS is essential for the development of novel approaches to treat MDD. Most mGlu<sub>2</sub> and mGlu<sub>3</sub> ligands interact with both receptors, and the development of compounds that selectively target one subtype has proven difficult. For this reason, our understanding of how mGlu<sub>2</sub> and mGlu<sub>3</sub> individually modulate PFC neurotransmission and produce antidepressant-like effects remains inadequate. Recently, our lab has developed highly selective and systemically active negative allosteric modulators (NAMs) for both mGlu<sub>2</sub> and mGlu<sub>3</sub>, devoid of activity at all other mGlu receptor subtypes and a large panel of clinically relevant targets (Bollinger et al., 2017; Engers et al., 2015). These compounds have been extensively validated in functional studies using constitutive genetic deletion of mGlu<sub>2</sub> or mGlu<sub>3</sub> (Di Menna et al., 2018). Availability of mGlu<sub>2</sub> and mGlu<sub>3</sub> selective molecular probes now permits us to test the hypothesis that selective inhibition of mGlu<sub>2</sub> or mGlu<sub>3</sub> enhances PFC glutamate transmission and confers antidepressant efficacy in preclinical models.

Here, we rigorously examined the effects of mGlu<sub>2</sub> and mGlu<sub>3</sub> NAM administration on excitatory transmission in the PFC. We found that systemic treatment with either an mGlu<sub>2</sub> NAM or mGlu<sub>3</sub> NAM enhances c-Fos expression in PFC pyramidal cells with pronounced hyperpolarization sag and larger and more frequent excitatory postsynaptic currents (EPSCs) relative to neighboring neurons. Several studies have found that PFC pyramidal cells with these biophysical properties (often denoted

“type A” neurons) preferentially project to subcortical structures and display strong reciprocal connections with the mediodorsal nucleus of the thalamus (MDT) (Anastasiades et al., 2018; Collins et al., 2018). Transmission from the MDT to the PFC has previously been implicated in antidepressant-like behavioral effects (An et al., 2017; Miller et al., 2017). Therefore, we used optogenetics to isolate this circuit and found that mGlu<sub>2</sub> constitutively gates MDT-PFC glutamate release probability and that both mGlu<sub>2</sub> and mGlu<sub>3</sub> regulate LTD at these synapses. Consistent with these physiological actions, both mGlu<sub>2</sub> and mGlu<sub>3</sub> NAMs decreased passive coping behavior in the forced swim test. Finally, we demonstrated that a single treatment with either an mGlu<sub>2</sub> or an mGlu<sub>3</sub> NAM reverses anhedonia in independent homotypic and heterotypic chronic stress models. Together, these data suggest that both mGlu<sub>2</sub> and mGlu<sub>3</sub> NAMs merit continued investigation for their potential utility as rapid-acting antidepressant treatments for MDD.

## RESULTS

### Systemic mGlu<sub>2</sub> and mGlu<sub>3</sub> NAM Administration Activates PFC Neuronal Ensembles with Relatively High Synaptic Strength

Stimulation of glutamate transmission in the PFC is essential for the antidepressant-like efficacy of mGlu<sub>2/3</sub> antagonists (Fukumoto et al., 2016). In addition, systemic treatment with mGlu<sub>2/3</sub> antagonists robustly increases c-Fos expression in the PFC in both mGlu<sub>2</sub> and mGlu<sub>3</sub> knockout mice (Hetzenauer et al., 2008; Linden et al., 2005). To examine how selective mGlu<sub>2</sub> and mGlu<sub>3</sub> NAMs induce PFC c-Fos induction, we systemically administered vehicle, the mGlu<sub>2</sub> NAM VU6001966 (10 mg/kg, intraperitoneally [i.p.]; Bollinger et al., 2017), or the mGlu<sub>3</sub> NAM VU0650786 (30 mg/kg, i.p.; Engers et al., 2015; Joffe et al., 2019a) to transgenic *cfos-EGFP* mice 45 min prior to slice preparation (Figure 1A). Doses were selected to achieve unbound brain concentrations 3 times higher than each NAM's IC<sub>50</sub> (Bollinger et al., 2017; Engers et al., 2015). We observed c-Fos induction following NAM administration throughout all layers of the PFC (Figure 1B) and then performed a quantitative cell count across random samples within layer 5. In vehicle-treated mice, approximately 10% of PFC cells exhibited detectable c-Fos labeling (Figures 1C and 1D). Following administration of either mGlu<sub>2</sub> or mGlu<sub>3</sub> NAM, the proportion of c-Fos-positive cells increased roughly 4-fold, suggesting that inhibition of either receptor subtype can elicit robust activation of the PFC.

To assess the mechanisms through which mGlu<sub>2</sub> and mGlu<sub>3</sub> NAMs recruit PFC neuronal ensembles, we prepared acute slices of *cfos-EGFP* mice for whole-cell electrophysiology and assessed membrane and synaptic properties in targeted GFP(+) and GFP(−) pyramidal cells in layer 5 prelimbic (PL)-PFC (Figure 2A). Overall, there were minimal effects of NAM treatment or c-Fos-GFP expression on pyramidal cell membrane properties (Figure S1). Following mGlu<sub>2</sub> and mGlu<sub>3</sub> NAM treatment, however, we observed a larger hyperpolarization sag in GFP(+) neurons relative to GFP(−) neurons in the same slices (Figures 2B and 2C), consistent with greater function of hyperpolarization-activated cyclic nucleotide-gated (HCN) channels in ensembles activated by systemic NAM administration (Thuault

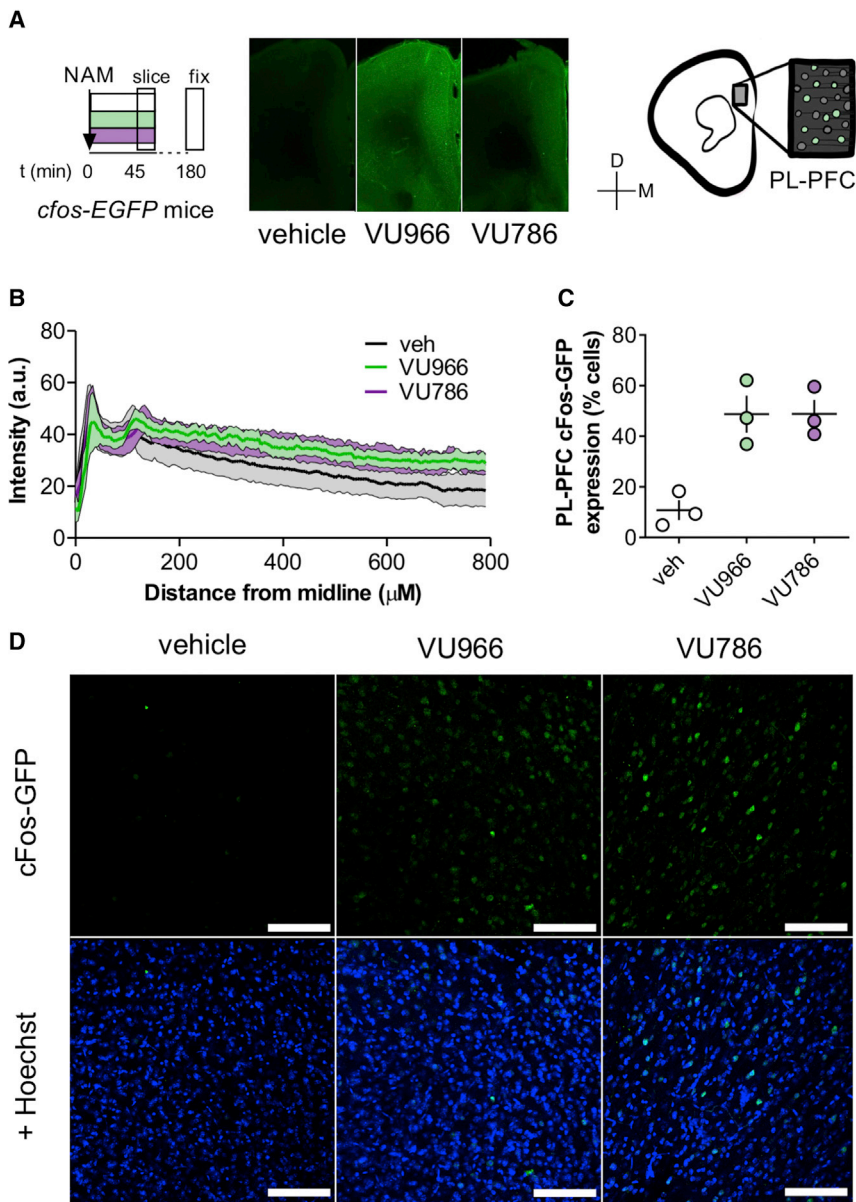


**Figure 1. Systemic Administration of Either mGlu<sub>2</sub> or mGlu<sub>3</sub> NAM Rapidly Activates the Mouse PFC**

(A) *cFos-EGFP* mice received vehicle, the mGlu<sub>2</sub> NAM VU6001966 (VU966) (10 mg/kg), or the mGlu<sub>3</sub> NAM VU0650786 (VU786) (30 mg/kg) 45 min prior to sacrifice for slice preparation, fixation, and processing for immunohistochemistry. Representative coronal widefield images displaying GFP expression throughout several medial PFC areas following NAM administration are shown.

(B) GFP expression throughout all layers of the medial PFC.

(C) Prelimbic PFC slices from NAM-treated mice displayed robust increases in the proportion of GFP-expressing cells.  $N = 3$  mice per group with 2–4 replicates per mouse.

(D) Representative images of GFP expression (top) and co-localization with Hoechst nuclear stain used for the quantification in (D). Scale bars represent 100  $\mu\text{m}$ .

Error bars represent SEM.

et al., 2013). In vehicle-treated mice, we observed no difference in the amplitude or frequency of AMPA-receptor-mediated spontaneous excitatory postsynaptic currents (sEPSCs) in GFP(+) or GFP(–) cells (Figures 2D–2F). By contrast, systemic treatment with either the mGlu<sub>2</sub> NAM or mGlu<sub>3</sub> NAM was associated with significantly greater sEPSC amplitude (Figure 2D) and frequency (Figure 2E) in *c-Fos-GFP*-expressing PFC neuronal ensembles relative to nearby GFP(–) pyramidal cells.

These findings raise two, non-exclusive possible explanations: (1) mGlu<sub>2</sub>/mGlu<sub>3</sub> NAM treatment rapidly enhances HCN channel function and synaptic strength and (2) mGlu<sub>2</sub>/mGlu<sub>3</sub> NAM treatment activates pyramidal cell ensembles with pre-existing large sag and synaptic strength. For an initial assessment, we plotted the relationship between hyperpolarization sag and sEPSC amplitude and frequency for each cell (Figures 2G and

2H). This analysis revealed positive correlations between sag ratio and sEPSC amplitude and frequency. Interestingly, the correlation between sag ratio and sEPSC amplitude was present in controls (Figure S2B), supporting the hypothesis that mGlu<sub>2</sub>/mGlu<sub>3</sub> NAMs activate a pre-existing subpopulation with the intrinsic and synaptic properties of type A pyramidal cells. On the other hand, the effect on sEPSC frequency emerged only after NAM treatment (Figure S2C), suggesting mGlu<sub>2</sub> and mGlu<sub>3</sub> NAMs might inherently increase synaptic strength in a subset of pyramidal cells.

### mGlu<sub>2</sub> NAMs Enhance Thalamic Cortical Glutamate Release Probability

To test whether mGlu<sub>2</sub> and mGlu<sub>3</sub> inhibition directly enhance HCN channel function

and sEPSCs, we incubated acute PFC slices with vehicle (0.1% DMSO), VU6001966 (3  $\mu\text{M}$ ), or VU0650786 (10  $\mu\text{M}$ )—concentrations 30-fold higher than the  $\text{IC}_{50}$  evaluated in heterologous systems (Bollinger et al., 2017; Engers et al., 2015)—and recorded from unlabeled, randomly sampled pyramidal cells (Figure 3A). We observed minimal effects on membrane physiology (Figure S3), including the hyperpolarization sag (Figures 3B and 3C), suggesting that mGlu<sub>2</sub>/mGlu<sub>3</sub> NAMs do not alter HCN channel function but that systemic NAM administration activates pyramidal cell ensembles with distinct pre-existing membrane properties. By contrast, slice treatment with the mGlu<sub>2</sub> NAM VU6001966, but not the mGlu<sub>3</sub> NAM VU0650786, increased both sEPSC amplitude (Figure 3D) and frequency (Figure 3E), indicating that mGlu<sub>2</sub> NAMs can rapidly increase PFC glutamate transmission, even in a

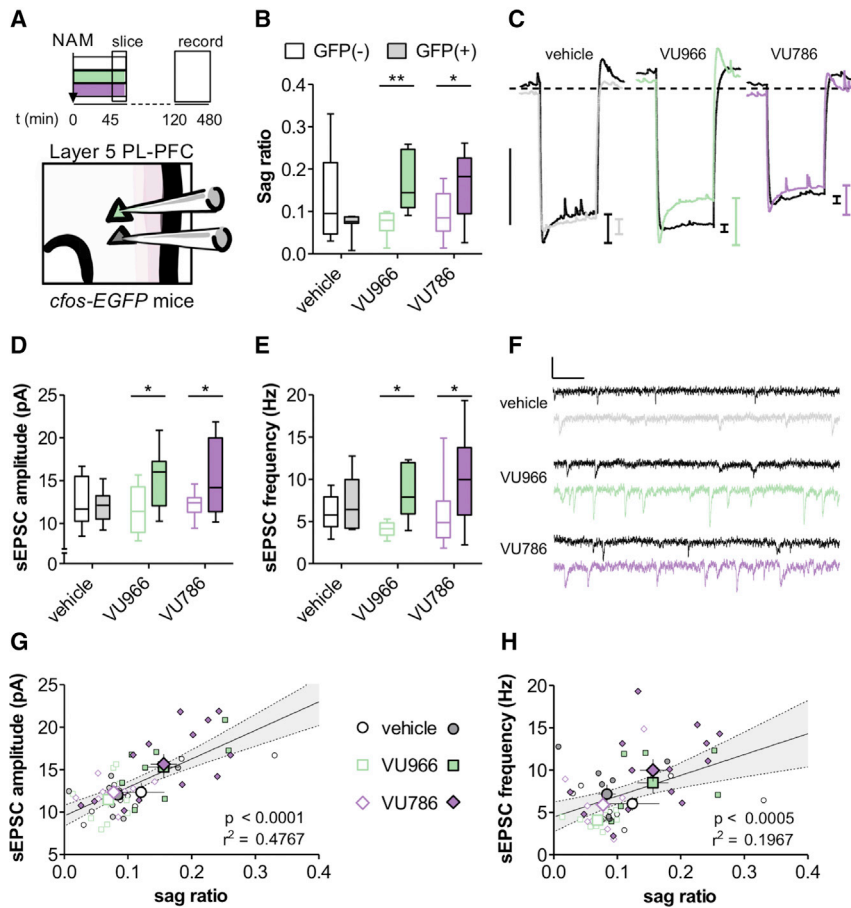


**Figure 2. PFC Neuronal Ensembles Activated by mGlu<sub>2</sub> or mGlu<sub>3</sub> NAMs Exhibit Large Hyperpolarization Sag and High Synaptic Strength**

(A) *cFos-EGFP* mice were administered vehicle, mGlu<sub>2</sub> NAM VU6001966 (10 mg/kg), or mGlu<sub>3</sub> NAM VU0650786 (30 mg/kg) 45 min prior to being sacrificed for slice electrophysiology. Whole-cell patch-clamp recordings from targeted GFP(+) and GFP(-) pyramidal cells in layer 5 prelimbic PFC were made 1–6 h after slice preparation.

(B) GFP(+) neuronal ensembles display relatively high hyperpolarization sag relative to neighboring GFP(-) pyramidal cells (two-way ANOVA trend effect of Fos-GFP:  $F_{1,55} = 3.69$ ,  $p < 0.06$ ; significant effect of Fos-GFP  $\times$  NAM interaction:  $F_{2,55} = 6.99$ ,  $p < 0.01$ ;  $*p < 0.05$ ;  $**p < 0.01$ ; Bonferroni post-test versus GFP(-)).  $n/N = 8-14/3-4$  cells/mice per group.

(C) Representative traces of negative current injections. Scale bars indicate 10 mV. Dashed line indicates  $-70$  mV.

(D) GFP(+) neuronal ensembles exhibited relatively large sEPSC amplitude following systemic NAM treatment (main effect of Fos-GFP:  $F_{1,52} = 8.0$ ,  $p < 0.01$ ;  $*p < 0.05$ ; Bonferroni post-test versus GFP(-)).  $n/N = 8-13/3-4$  cells/mice.

(E) GFP(+) neuronal ensembles displayed enhanced sEPSC frequency (main effect of Fos-GFP:  $F_{1,52} = 11.5$ ,  $p < 0.002$ ;  $*p < 0.05$ , Bonferroni post-test versus GFP(-)).  $n/N = 8-13/3-4$ .

(F) Representative sEPSC recordings. Scale bars indicate 20 pA and 100 ms.

(G) Positive correlation between sEPSC amplitude and sag ratio.

(H) Positive correlation between sEPSC frequency and sag ratio.

Error bars represent SEM. Box plots display median, interquartile range, and range.

reduced system. There was no association between the duration of NAM incubation and synaptic strength (Figure S4). Finally, we replicated the correlation between sag ratio and sEPSC amplitude (Figure 3G) in PFC pyramidal cells, consistent with a pre-existing subpopulation of pyramidal cells particularly responsive to mGlu<sub>2</sub>/mGlu<sub>3</sub> NAM treatment. Importantly, the correlation does not stem from cell-to-cell variation in access resistance (Figure S3). Altogether, these findings indicate that systemic treatment with mGlu<sub>2</sub> and mGlu<sub>3</sub> NAMs rapidly but divergently activates neuronal ensembles in the PFC with relatively large sag ratios and post-synaptic strength. Finally, we observed no correlation between sag ratio and sEPSC frequency following slice incubation (Figure 3H), consistent with the data collected from vehicle-treated, *cFos-EGFP* mice (Figure S2). Together, these data suggest that mGlu<sub>2</sub> and mGlu<sub>3</sub> NAMs must recruit phasic PFC transmission to enhance quantal content. Based on this, we evaluated how mGlu<sub>2</sub> and mGlu<sub>3</sub> regulate evoked, long-range glutamate transmission in the PFC.

PFC pyramidal cells with large hyperpolarization sag tend to target subcortical structures, particularly the MDT (Anastasiades et al., 2018; Collins et al., 2018). These neurons, in turn, receive strong reciprocal input from the MDT, and this circuit appears to be particularly important in promoting antidepressant-like responses in rodent models and MDD

patients (An et al., 2017; Miller et al., 2017). Based on these studies, we set out to test the hypothesis that mGlu<sub>2</sub> and mGlu<sub>3</sub> NAMs enhance MDT-PFC glutamate transmission. To isolate MDT-PFC synaptic transmission, we virally expressed the optogenetic protein Chr2 in the MDT and made PFC slice recordings from adult mice (Figure 4A). Acute application of the mGlu<sub>2/3</sub> antagonist LY341495 (200 nM) increased the amplitude of the MDT-PFC optical (op)-EPSC (Figures 4B and 4D), suggesting that mGlu<sub>2</sub> and/or mGlu<sub>3</sub> tonically restrain thalamocortical transmission. To assess the involvement of individual receptor subtypes, we bath applied the mGlu<sub>2</sub> NAM VU6001966 or the mGlu<sub>3</sub> NAM VU0650786 in separate slices. Interestingly, VU6001966, but not VU0650786, enhanced the evoked op-EPSC (Figures 4C and 4D), suggesting that only mGlu<sub>2</sub> constitutively inhibits basal MDT-PFC transmission. Similar findings were obtained with electrical stimulation (Figure S5). To examine the synaptic locus of action of these effects, we measured the MDT-PFC PPR after extended NAM application. PPR was decreased in the presence of VU6001966, but not VU0650786 (Figures 4E and 4F), consistent with an increase in presynaptic release probability. Taken together, these data suggest that inhibition of mGlu<sub>2</sub> autoreceptors increases thalamocortical glutamate release probability, whereas mGlu<sub>3</sub> receptors do not function in this manner.

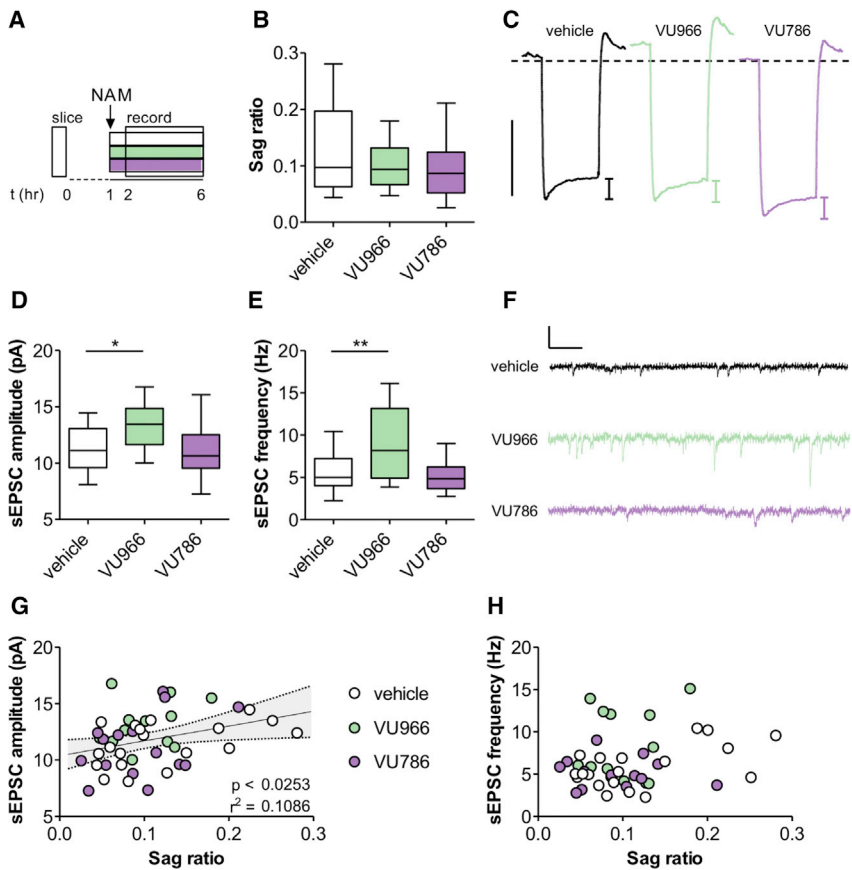


### Figure 3. mGlu<sub>2</sub> Inhibition in Acute PFC Slices Increases Excitatory Synaptic Strength

(A) PFC slices were prepared and incubated with vehicle, mGlu<sub>2</sub> NAM VU6001966 (3 μM), or mGlu<sub>3</sub> NAM VU0650786 (10 μM) for 1–6 h prior to whole-cell recordings.

(B) No effect of slice NAM treatment on hyperpolarization sag (ANOVA main effect of NAM:  $F_{2,44} = 1.7$ ;  $p < 0.27$ ;  $n/N = 12\text{--}20/4$  cells/mice per group).

(C) Representative traces displaying membrane hyperpolarization in response to a 150-pA hyperpolarizing current. Scale bar represents 10 mV. Dashed line indicates  $-70$  mV.

(D and E) Incubation with the mGlu<sub>2</sub> NAM, but not the mGlu<sub>3</sub> NAM, increased sEPSC amplitude ( $F_{2,44} = 2.3$ ,  $p < 0.04$ ,  $n/N = 13\text{--}19/4$ ; \* $p < 0.05$  Bonferroni post-test versus vehicle) and frequency ( $F_{2,43} = 11.98$ ,  $p < 0.0034$ ,  $n/N = 13\text{--}19/4$ ; \*\* $p < 0.01$  Bonferroni post-test versus vehicle).

(F) Representative sEPSC traces. Scale bars indicate 20 pA and 100 ms.

(G) Positive correlation between sEPSC amplitude and hyperpolarization sag.

(H) No correlation between sEPSC frequency and sag ratio.

Error bars represent SEM. Box plots display median, interquartile range, and range.

### Both mGlu<sub>2</sub> and mGlu<sub>3</sub> NAMs Attenuate Thalamocortical LTD

Our lab has demonstrated that activation of mGlu<sub>3</sub>, and not mGlu<sub>2</sub>, induces robust LTD in the PFC with respect to electrically evoked EPSCs or when isolating inputs from the basolateral amygdala (BLA) (Di Menna et al., 2018; Joffe et al., 2019a). These studies revealed that mGlu<sub>3</sub>-LTD is expressed postsynaptically and requires the activation of phosphoinositide 3-kinase, Akt, and the internalization of AMPA receptors (Joffe et al., 2019a, 2019b). Here, we aimed to address LTD at specific afferents from the MDT. As with the wash-on experiments, acute PFC-containing brain slices were made from adult mice several weeks following viral expression of ChR2 in the MDT (Figure 5A). As with our previous studies, we applied the mGlu<sub>2/3</sub> agonist LY379268 for 10 min to induce LTD at MDT-PFC synapses (Figures 5B and 5C). Immediately, we noticed that the magnitude of MDT-PFC LTD was greater than we previously observed with electrical or BLA-specific stimulation. To identify the specific mGlu receptor subtypes involved in this LTD, we pre-applied either VU6001966 or VU0650786. NAMs or the mGlu<sub>2/3</sub> antagonist were delivered for at least 30 min prior to LTD induction to mitigate the potential effect of increased glutamate release. Unlike our results with electrical or BLA-specific stimulation (Joffe et al., 2019a), the mGlu<sub>2</sub> NAM impaired the magnitude of LTD (Figure 5D), indicating a role for mGlu<sub>2</sub> in LTD induction at thalamocortical synapses. To corroborate the involvement of mGlu<sub>2</sub> in MDT-PFC LTD, we replicated this experiment using a sepa-

rate, structurally distinct mGlu<sub>2</sub> NAM, MRK-8-29 (Walker et al., 2015), and a selective mGlu<sub>2</sub> partial agonist (Figure S5D). We followed these experiments with VU0650786 (Figure 5E). The mGlu<sub>3</sub> NAM also impaired LTD; however, unlike experiments using electrically evoked or BLA-specific glutamate release, a considerable decrease in synaptic strength remained after this manipulation. Because we observed partial blocks with either mGlu<sub>2</sub> or mGlu<sub>3</sub> NAM, we performed additional experiments using LY341495 to corroborate that only mGlu<sub>2</sub> and mGlu<sub>3</sub> mediate MDT-PFC LTD. Indeed, LY341495 completely blocked the induction of LTD (Figure 5F). A comparative analysis across the last 10 min of the recordings reveals that mGlu<sub>2</sub> and mGlu<sub>3</sub> each contribute comparably to LTD at MDT-PFC synapses (Figure 5G). Whether by modulation of presynaptic release probability or by inhibiting LTD, these data suggest that NAMs of either receptor could potentiate thalamocortical transmission *in vivo*. We therefore reasoned that both mGlu<sub>2</sub> and mGlu<sub>3</sub> NAMs would exert antidepressant-like behavioral effects and set out to test this hypothesis.

### mGlu<sub>2</sub> and mGlu<sub>3</sub> NAMs Decrease Passive Coping in an Acute Antidepressant Model

The forced swim test is routinely used to assess the behavioral actions of potential antidepressant treatments, whereby antidepressants prolong active coping mechanisms and increase the latency to enter a passive, immobile, floating posture. To assess the potential antidepressant-like action of mGlu<sub>2</sub> and mGlu<sub>3</sub> NAMs, we systemically delivered VU6001966 or VU0650786 to mice 45 min prior to performing the forced swim test (Figure 6A). Acute treatment with either VU6001966

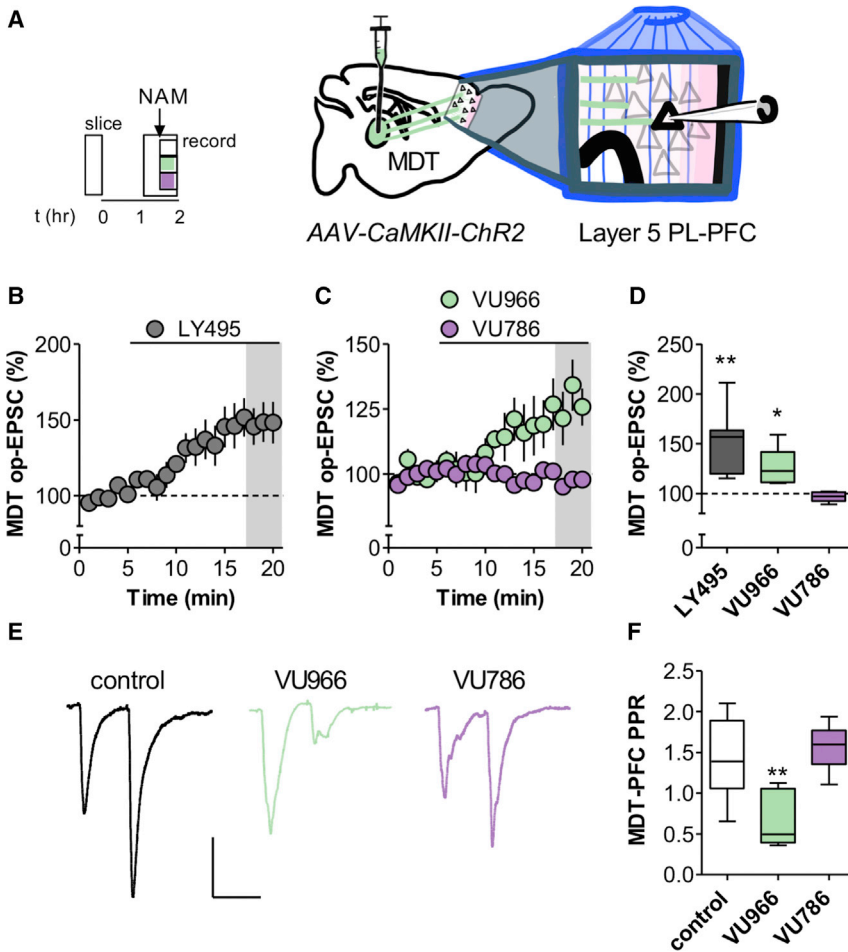


**Figure 4. mGlu<sub>2</sub> NAMs Enhance Glutamate Release Probability at Thalamocortical Synapses**

(A) ChR2 was expressed in the MDT of young mice. Acute brain slices containing the PFC were prepared 3–5 weeks later, and op-EPSCs were elicited on layer 5 PFC pyramidal cells.

(B) Bath application of LY341495 (LY495) (200 nM), an mGlu<sub>2/3</sub> orthosteric antagonist, enhanced thalamocortical transmission (150% ± 13% baseline; n/N = 7/4 cells/mice per group).

(C) Bath application of mGlu<sub>2</sub> NAM VU6001966 (3 μM), an mGlu<sub>2</sub> NAM, enhanced thalamocortical transmission (127% ± 8% baseline; n/N = 6/4), whereas mGlu<sub>3</sub> NAM VU0650786 (10 μM) did not (97% ± 2% baseline; n/N = 6/4).

(D) Summary of last 3 min of each recording (\*p < 0.05; \*\*p < 0.01; one-sample test versus 100%).

(E) Representative traces of MDT-PFC op-EPSCs; scale bars represent 100 pA and 50 ms. EPSCs were elicited with a 50-ms interstimulus interval, and the paired-pulse ratio (PPR) was obtained by normalizing the amplitude of the second pulse to the first.

(F) Extended slice incubation with VU6001966 decreased the MDT-PPR (ANOVA main effect of NAM:  $F_{2,20} = 10.1$ ,  $p < 0.001$ ; \*\*p < 0.01, Bonferroni post-test versus control, n/N = 6–11/4–6).

Error bars represent SEM. Box plots display median, interquartile range, and range.

or VU0650786 increased the latency to float immobile and decreased the total time of immobility (Figures 6B and 6C). We also performed studies in the tail suspension test (Figure 6D), an operationally similar assay that takes advantage of a mouse's instinct to right itself when suspended upside down. We previously reported no effect of mGlu<sub>2</sub> NAM administration on immobility in the tail suspension test in CD1 mice at doses up to 30 mg/kg (Engers et al., 2017). In agreement with those findings, acute treatment with the mGlu<sub>2</sub> NAM VU6001966 did not attenuate passive coping behavior in C57BL/6J mice following tail suspension (Figures 6E and 6F). In contrast, administration of the mGlu<sub>3</sub> NAM VU0650786 increased escape behavior and decreased passive coping in the tail suspension. Importantly, neither VU6001966 nor VU0650786 enhance locomotor activity 45 min after their administration (Figure S6), although the mGlu<sub>2</sub> NAM VU6001966 decreased locomotion immediately after injection. Together, these data suggest that both mGlu<sub>2</sub> and mGlu<sub>3</sub> NAMs decrease passive coping in acute models of antidepressant-like activity. In addition, mGlu<sub>2</sub> NAMs may preferentially exert efficacy under conditions that alter systemic stress hormone levels (Solich et al., 2008), although the task-dependent efficacy of VU6001966 may be better explained by other variables (Cryan et al., 2005).

an intersectional chemogenetic approach (Vardy et al., 2015). To that end, we virally expressed the G<sub>i</sub>-coupled κ opioid receptor DREADD (KORD) in MDT neurons that project to the PFC (Figure 7A). Application of the specific KORD agonist salvinorin B (SALB) inhibited the MDT op-EPSC in PFC pyramidal cells without affecting EPSCs evoked with electrical stimulation (Figure 7B). We next asked whether inhibiting MDT-PFC transmission *in vivo* would affect the efficacy of the VU6001966 and VU0650786 in the forced swim test. Mice expressing KORD in the MDT-PFC pathway received vehicle, the mGlu<sub>2</sub> NAM VU6001966, or the mGlu<sub>3</sub> NAM VU0650786 45 min before the forced swim. Then, 10 min before the test, mice received an additional injection with DMSO or SALB (10 mg/kg) (Figure 7C). Relative to DMSO/vehicle-treated controls, VU6001966 and VU0650786 each prolonged the latency to immobility (Figure 7D). In the group that received the KORD agonist SALB, however, there were no differences between vehicle, VU6001966, and VU0650786 treatment, although we did observe a trend increase in latency to immobility in vehicle-SALB mice. Importantly, chemogenetic inhibition of MDT-PFC transmission did not modulate locomotor activity (Figure S7), and SALB did not modulate passive coping in control mice not expressing KORD (Figure 7D). Although these data do not conclusively exclude the involvement of other neurocircuits, they suggest that changes in MDT-PFC

### MTD-PFC Inhibition Prevents Antidepressant-like Effect of mGlu<sub>2</sub>/mGlu<sub>3</sub> NAMs

To test whether modulation of MDT-PFC transmission underlies the behavioral efficacy of mGlu<sub>2</sub>/mGlu<sub>3</sub> NAMs, we employed

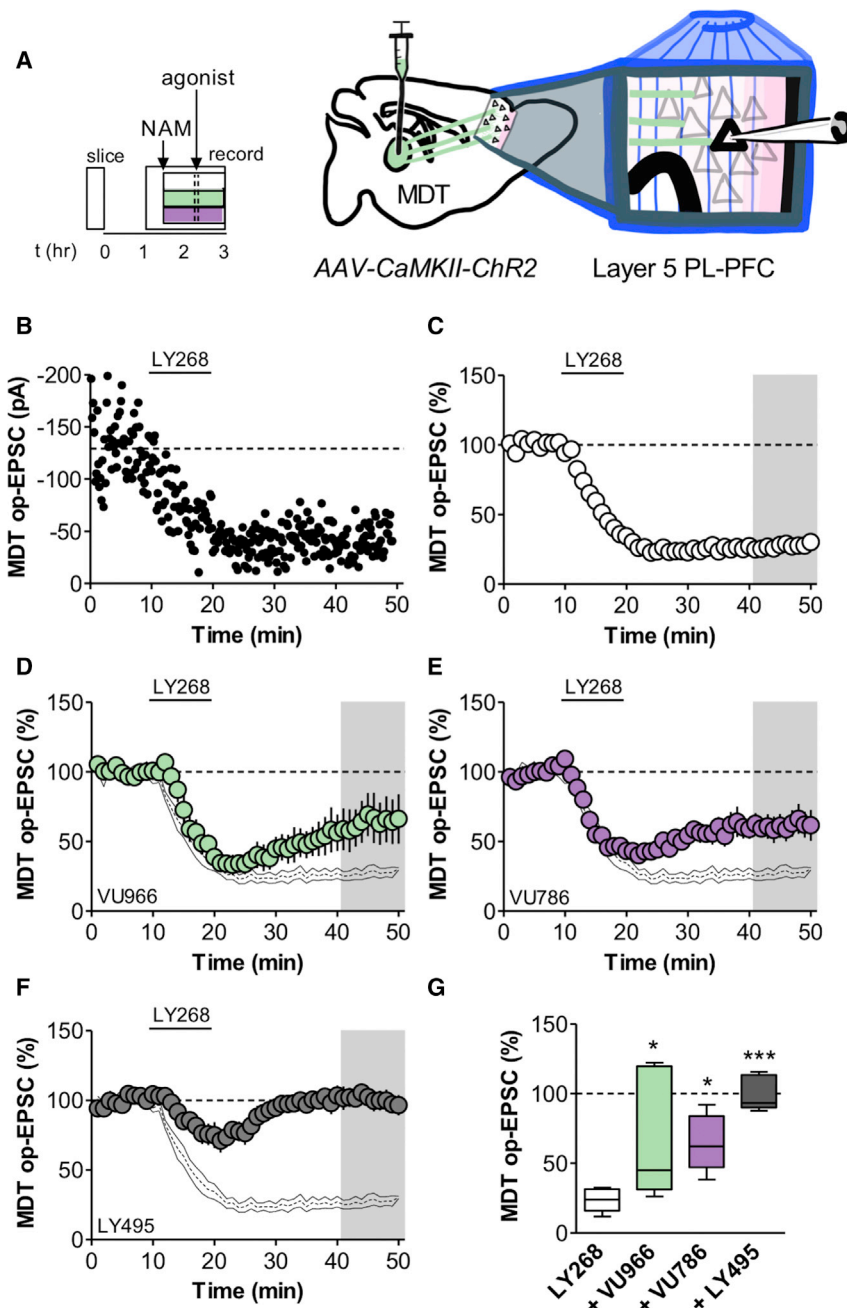


### Figure 5. mGlu<sub>2</sub> and mGlu<sub>3</sub> NAMs Attenuate LTD at Thalamocortical Synapses

(A) A virus promoting the expression of Chr2 was injected into the MDT of young mice. Acute brain slices containing the PFC were prepared 3–5 weeks later, and op-EPSCs were elicited on isolated layer 5 PFC pyramidal cells.

(B) Representative experiment illustrating LTD at thalamocortical synapses following bath application of LY379268 (LY268) (200 nM), an mGlu<sub>2/3</sub> orthosteric agonist.

(C) Averaged time courses showing robust LTD at MDT-PFC synapses (24% ± 3% baseline; n/N = 7/6 cells/mice per group).

(D) mGlu<sub>2</sub> NAM VU6001966 (3 μM), an mGlu<sub>2</sub> NAM, partially inhibited LTD (64% ± 15% baseline; n/N = 7/3). Black lines display control data from (C).

(E) mGlu<sub>3</sub> NAM VU0650786 (10 μM) partially inhibited LTD induction (64% ± 8% baseline; n/N = 6/4).

(F) Bath application of LY341495, an mGlu<sub>2/3</sub> orthosteric antagonist, completely blocked LTD expression (100% ± 6% baseline; n/N = 5/2).

(G) Summary of last 10 min of each recording (ANOVA main effect of drug:  $F_{3,21} = 9.3$ ,  $p < 0.004$ ; \* $p < 0.05$ , \*\*\* $p < 0.001$ , Bonferroni post-test versus control).

Error bars represent SEM. Box plots display median, interquartile range, and range.

neurotransmission contribute to the antidepressant-like effects of mGlu<sub>2</sub> and mGlu<sub>3</sub> NAMs.

### Both mGlu<sub>2</sub> and mGlu<sub>3</sub> NAMs Reverse Chronic-Stress-Induced Anhedonia

Acute tests of escape behavior are predictive of antidepressant-like mechanisms of action; however, chronic stress models provide substantially greater translational value in terms of their construct validity and ability to detect rapid-acting antidepressants. We therefore set out to assess whether mGlu<sub>2</sub> or mGlu<sub>3</sub> NAMs could reverse anhedonia, an MDD symptom that is poorly managed by available treatments. We first modeled chronic

stress exposure following chronic treatment with the stress hormone corticosterone (CORT), a manipulation known to alter PFC function and induce depressive-like phenotypes in rodent models (Gourley et al., 2008b; Wellman, 2001; Yuen et al., 2012). We delivered CORT in 0.5% beta-cyclodextrin (β-CD) in the drinking water for 4 weeks and performed behavioral experiments 1 week later (Figure 8A). Consistent with previous studies in C57BL/6J mice (Gourley et al., 2008a; Sturm et al., 2015), CORT-treated mice displayed a significant reduction in sucrose preference and decreased weight gain relative to mice given the β-CD vehicle (Figure S8A). We next assessed whether mGlu<sub>2</sub> or mGlu<sub>3</sub> NAMs can rapidly reverse CORT-induced anhedonia, an effect that is refractory

to acute treatment with conventional antidepressants. The day prior to behavioral testing, we administered vehicle, VU6001966, or VU0650786 to a separate cohort of CORT-treated mice. The next day, vehicle-treated mice displayed no preference for sucrose over water, but strikingly, acute treatment with either VU6001966 or VU0650786 reversed this anhedonic phenotype (Figure 8B). We then examined escape behavior in the forced swim and tail suspension tests. Both mGlu<sub>2</sub> and mGlu<sub>3</sub> NAMs decreased passive coping in the forced swim test (Figure 8C), and unlike the experiment in control mice, both VU6001966 and VU0650786 increased the latency to hang immobile in the tail suspension test in CORT-treated mice (Figure 8D).

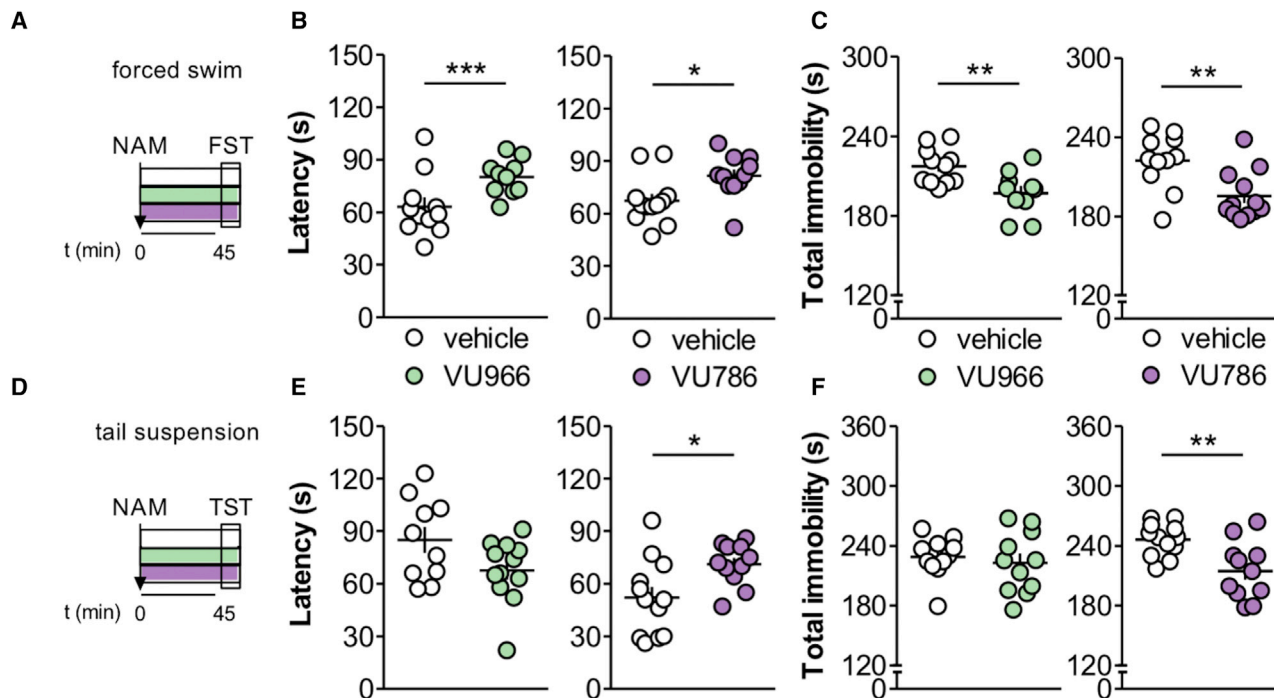


**Figure 6. mGlu<sub>2</sub> and mGlu<sub>3</sub> NAMs Decrease Passive Coping in Acute Antidepressant Models**

(A) A selective mGlu receptor NAM, or its vehicle, was administered 45 min prior to the forced swim test (FST).

(B) mGlu<sub>2</sub> NAM VU6001966 (10 mg/kg) and mGlu<sub>3</sub> NAM VU0650786 (30 mg/kg) each increased the latency to immobility in the FST (\**p* < 0.05; \*\*\**p* < 0.001; *t* test versus vehicle). *N* = 11–12 mice per group.

(C) VU6001966 and VU0650786 each decreased total time spent immobile in the FST (\*\**p* < 0.01; *t* test versus vehicle).

(D) A selective mGlu receptor NAM, or its vehicle, was administered 45 min prior to the tail suspension test (TST).

(E) VU0650786, but not VU6001966, increased latency to immobility in the TST (\**p* < 0.05; *t* test versus vehicle). *N* = 10–12.

(F) VU0650786, but not VU6001966, decreased total immobility in the TST (\*\**p* < 0.01; *t* test versus vehicle).

Error bars represent SEM.

In addition to chronic CORT treatment, a model of homotypic stress, we examined whether mGlu<sub>2</sub> or mGlu<sub>3</sub> NAMs can reverse anhedonia following heterotypic stress, which may more accurately model the pathophysiology of MDD. To that end, we implemented a chronic variable stress (CVS) model, whereby mice were presented with six “mild” stressors in a variable order over a 4-week period (Figure 8E). As with the CORT model, CVS mice displayed decreased sucrose preference and weight gain relative to controls (Figure S8B), and we then assessed sucrose preference 1 day after a single treatment with vehicle, VU6001966, or VU0650786. As with the CORT-treated mice, sucrose preference in CVS mice was restored following one treatment with either mGlu<sub>2</sub> or mGlu<sub>3</sub> NAM (Figure 8F). Moreover, VU0650786 retained antidepressant-like efficacy in both the forced swim and tail suspension tests (Figures 8G and 8H). VU6001966 increased the latency to immobility in the tail suspension test but did not reach significance in the forced swim test in this cohort. Together, these data indicate that selective NAMs for both mGlu<sub>2</sub> and mGlu<sub>3</sub> can rapidly reverse anhedonia in independent preclinical chronic stress models. Overall the behavioral findings suggest that selective mGlu<sub>2</sub> and mGlu<sub>3</sub> NAMs each display preclinical profiles comparable to mGlu<sub>2/3</sub> antagonists, ketamine, and other rapid-acting antidepressants.

## DISCUSSION

Orthosteric antagonists of mGlu<sub>2/3</sub> have been thoroughly evaluated in preclinical models of depressive-like behavior; however, the development of drug-like molecules that inhibit only one receptor subtype has been elusive (Chaki, 2017). A therapeutic approach requiring the inhibition of only one mGlu receptor subtype is expected to be advantageous due to decreased liability of undesirable side effects (Joffe and Conn, 2019). The recent discovery of potent, highly selective, and systemically active NAMs for both mGlu<sub>2</sub> and mGlu<sub>3</sub> provided the toolset for us to test whether inhibiting either receptor subtype alone recapitulates the preclinical efficacy of orthosteric antagonists. Because the efficacy of mGlu<sub>2/3</sub> antagonists and other rapid-acting antidepressants requires enhanced excitatory transmission in the PFC (Chaki, 2017), we first investigated the receptor subtypes and circuit mechanisms involved in PFC activation. Systemic treatment with either mGlu<sub>2</sub> or mGlu<sub>3</sub> NAMs increased c-Fos expression in pyramidal cells with prominent hyperpolarization sag and relatively large sEPSC amplitude and frequency. We found that both mGlu<sub>2</sub> and mGlu<sub>3</sub> NAMs enhanced thalamocortical transmission; however, mGlu<sub>2</sub> acts as a presynaptic autoreceptor whereas mGlu<sub>3</sub> serves alternative postsynaptic functions. Nonetheless, the physiological studies suggested that both

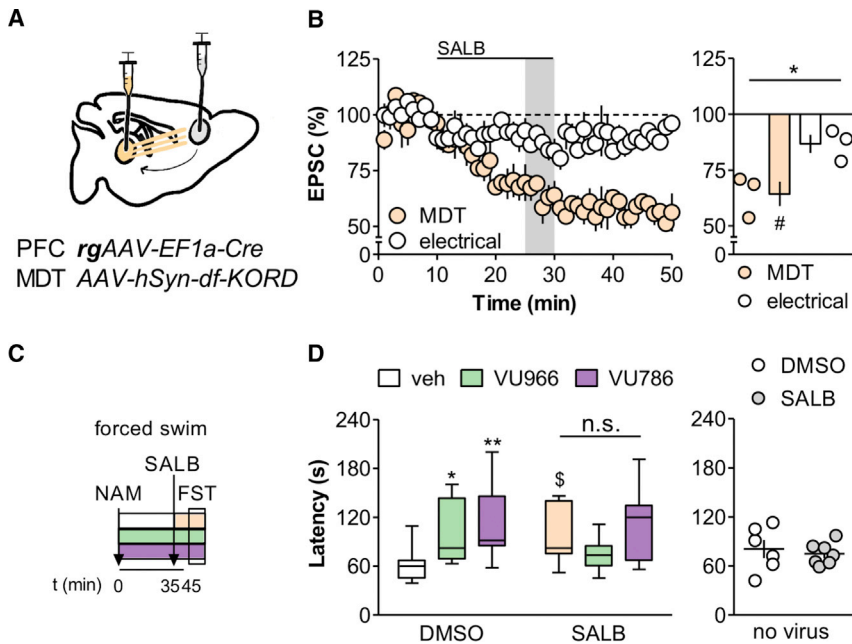


**Figure 7. MDT-PFC Inhibition Prevents Effects of mGlu<sub>2</sub> and mGlu<sub>3</sub> NAMs on Passive Coping Behavior**

(A) KORD was expressed in PFC-projecting MDT neurons, and acute PFC slices were prepared to validate KORD function at MDT-PFC synapses.

(B) The KORD agonist SALB (200 nM) selectively depressed glutamatergic transmission at MDT-PFC synapses (\* $p < 0.05$  paired t test; # $p < 0.05$ , one-sample t test versus 100%).  $n/N = 3/2$  slices/mice.

(C) mGlu<sub>2</sub> NAM VU6001966 (10 mg/kg), mGlu<sub>3</sub> NAM VU0650786 (30 mg/kg), or vehicle was administered 45 min prior to the FST. In combination, mice received SALB (10 mg/kg) or its vehicle DMSO 10 min prior to the FST.

(D) VU6001966 and VU0650786 did not modulate the latency to immobility in SALB-treated mice, whereas decreases in passive coping were intact in DMSO controls (two-way ANOVA main effect of NAM:  $F_{2,60} = 4.6$   $p < 0.02$ ; NAM  $\times$  SALB interaction:  $F_{2,60} = 3.877$   $p < 0.03$ ; \$ $p < 0.1$ , \* $p < 0.05$ , \*\* $p < 0.01$ , Bonferroni post-test versus DMSO/veh).  $N = 9-12$ . No effects on immobility were observed following SALB administration to control mice not expressing KORD.  $N = 6-7$ .

Error bars represent SEM. Box plots display median, interquartile range, and range.

receptors may promote activation of thalamocortical transmission *in vivo*, and consistent with these findings, both mechanisms increased antidepressant-like escape behavior. Finally, a single administration of either an mGlu<sub>2</sub> NAM or mGlu<sub>3</sub> NAM reversed anhedonia in two independent MDD-like chronic stress mouse models.

Increased glutamate transmission in the PFC is necessary and sufficient for the antidepressant-like effects of mGlu<sub>2/3</sub> antagonists (Fukumoto et al., 2016; Highland et al., 2019). In the current studies, we found evidence that both mGlu<sub>2</sub> and mGlu<sub>3</sub> receptors contribute to these effects, in that selective NAMs for both receptor subtypes increased c-Fos expression in the PFC, decreased passive coping in the forced swim test, and reversed anhedonia in two models of chronic stress. Although mGlu<sub>2/3</sub> antagonists rapidly induce PFC c-Fos expression (Linden et al., 2005), in a manner that depends on both mGlu<sub>2</sub> and mGlu<sub>3</sub> (Linden et al., 2009), discrepant expression patterns of the two receptor subtypes have long suggested that mGlu<sub>2</sub> and mGlu<sub>3</sub> receptors regulate distinct neurocircuits. Here, we isolated PFC inputs arising from the MDT and found that mGlu<sub>2</sub> and mGlu<sub>3</sub> NAMs differentially regulate thalamocortical transmission through distinct pre- and postsynaptic mechanisms. Consistent with these findings, mGlu<sub>2</sub> transcript is moderately expressed throughout the midline thalamic nuclei (Ohishi et al., 1993a), and mGlu<sub>2</sub>, but not mGlu<sub>3</sub>, also regulates thalamic glutamate release probability in the dorsal striatum (Johnson et al., 2017). By contrast, although mGlu<sub>3</sub> mRNA is abundantly expressed in the PFC and the reticular nucleus of the thalamus, it is virtually absent from the midline nuclei (Loureño Neto et al., 2000; Ohishi et al., 1993b). These findings strongly point toward postsynaptic mGlu<sub>3</sub> comprising the primary receptor subpopulation mediating mGlu<sub>3</sub> NAM-induced PFC activation and antidepressant-like activity, likely by regulating postsynaptically maintained synaptic plasticity (Joffe et al., 2019a, 2019b). Additionally, we note that

astrocytes and other glia express mGlu<sub>3</sub>, and further studies are warranted to examine how those receptor subpopulations may regulate PFC physiology and affective behaviors.

In the present studies, we leveraged inducible *cFos-EGFP* mice to thoroughly investigate the biophysical properties of neuronal ensembles activated by mGlu<sub>2</sub> and mGlu<sub>3</sub> NAM administration. This powerful approach provided a means to identify experience-related differences in intrinsic and synaptic properties that would be difficult to detect in groups of non-identified pyramidal cells. The specific phenotypes inherent to these NAM-activated neuronal ensembles were characterized by a predominant hyperpolarization sag and high synaptic strength. Two possible non-exclusive explanations could underlie this initial finding: (1) mGlu<sub>2</sub>/mGlu<sub>3</sub> NAMs increase PFC HCN channel function and synaptic strength and (2) activated neurons represent a subpopulation with high sag and synaptic strength prior to NAM administration. Further experiments revealed that mGlu<sub>2</sub> NAMs increase synaptic strength in acute PFC slices and that NAMs for both mGlu<sub>2</sub> and mGlu<sub>3</sub> block LTD at thalamocortical synapses. These findings suggest that systemic delivery of either mGlu<sub>2</sub> or mGlu<sub>3</sub> NAMs enhances MDT-PFC synaptic strength *in vivo*, consistent with the antidepressant-like effect observed in previous studies by manipulating this pathway with chemogenetics (Miller et al., 2017). Surprisingly, however, we observed that chemogenetic inhibition of the same pathway induced a trend antidepressant-like effect in the forced swim test. Given that MDT-PFC projections strongly activate fast-spiking interneurons (Delevich et al., 2015), one possible explanation is that MDT-PFC inhibition *in vivo* might induce net disinhibition of corticothalamic pyramidal cells.

Although mGlu<sub>2</sub> and mGlu<sub>3</sub> NAMs clearly enhance glutamate drive in the PFC, other evidence presented here suggests that some pyramidal cells display properties of NAM-activated ensembles prior to NAM administration. We observed a positive

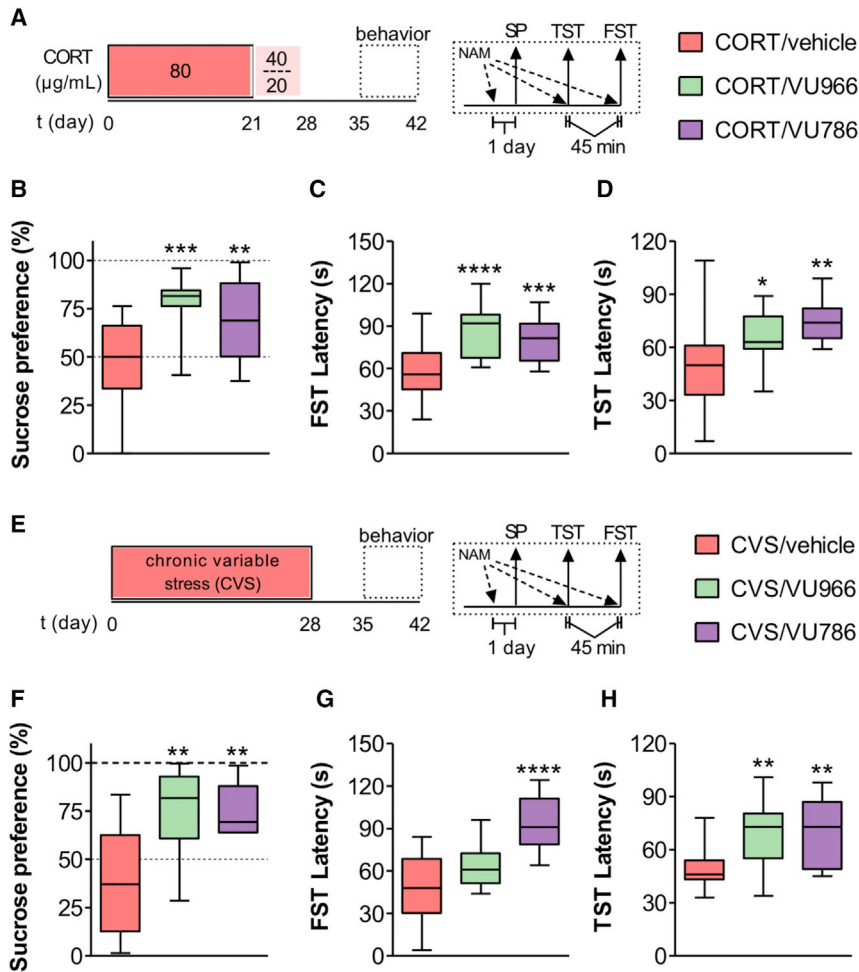


**Figure 8. mGlu<sub>2</sub> and mGlu<sub>3</sub> NAMs Each Reverse Chronic-Stress-Induced Anhedonia**

(A) Mice received the stress hormone CORT in the drinking water for 4 weeks. Behavioral studies were conducted 1 to 2 weeks after the cessation of CORT treatment. mGlu<sub>2</sub> NAM VU6001966 (10 mg/kg), mGlu<sub>3</sub> NAM VU0650786 (30 mg/kg), or vehicle was administered 24 h prior to the sucrose preference test and 45 min before the TST and FST. Behavioral assays were separated by 3 days, and mice remained in the same treatment group for all tests.

(B) Acute treatment with either VU6001966 or VU0650786 reversed CORT-induced anhedonia (ANOVA main effect of NAM:  $F_{2,50} = 10.4$ ,  $p < 0.0002$ ; \*\* $p < 0.01$ , \*\*\* $p < 0.001$ , Bonferroni post-test versus CORT/veh).  $N = 13$ –25 mice per group.

(C) Acute treatment with either VU6001966 or VU0650786 increased the latency to immobility in the FST in CORT-conditioned mice ( $F_{2,59} = 6.0$ ,  $p < 0.0001$ ; \*\*\* $p < 0.001$ , \*\*\*\* $p < 0.0001$ , Bonferroni post-test versus CORT/veh).  $N = 16$ –27.

(D) Acute treatment with either VU6001966 or VU0650786 increased the latency to immobility in the TST in CORT-treated mice ( $F_{2,52} = 7.8$ ,  $p < 0.002$ ; \* $p < 0.05$ , \*\* $p < 0.01$ , Bonferroni post-test versus CORT/veh).  $N = 11$ –25.

(E) Mice underwent CVS for 4 weeks, and behavioral studies were conducted 1 to 2 weeks after the cessation of CVS treatment.

(F) Acute treatment with either VU6001966 or VU0650786 reversed CVS-induced anhedonia ( $F_{2,25} = 8.9$ ,  $p < 0.002$ ; \*\* $p < 0.001$ , Bonferroni post-test versus CVS/veh).  $N = 6$ –11.

(G) Acute treatment with VU0650786 increased the latency to immobility in the FST in CVS-treated mice ( $F_{2,36} = 18.1$ ,  $p < 0.0001$ ; \*\*\*\* $p < 0.0001$ , Bonferroni post-test versus CVS/veh).  $N = 13$ .

(H) Acute treatment with either VU6001966 or VU0650786 increased the latency to immobility in the TST in CVS mice ( $F_{2,42} = 8.8$ ,  $p < 0.001$ ; \*\* $p < 0.01$ , Bonferroni post-test versus CVS/veh).  $N = 13$ . Box plots display median, interquartile range, and range.

correlation in two experimental cohorts between sag ratio and sEPSC amplitude, even in cells from vehicle-treated control groups. Furthermore, we found no evidence that mGlu<sub>2</sub>/mGlu<sub>3</sub> NAMs modify HCN channels function in randomly sampled, unlabeled pyramidal cells. These findings suggest that systemic mGlu<sub>2</sub> and mGlu<sub>3</sub> NAM administration activates specific pyramidal cell subsets with inherently large sag ratios and high synaptic strength. This conclusion begs the question, which pyramidal cell subtypes comprise these NAM-activated neuronal ensembles? Several studies have classified deep-layer PFC pyramidal cells with large sag ratios as type A neurons, which preferentially project to subcortical structures, including the MDT (Anastasiades et al., 2018; Collins et al., 2018). Relative to neighboring intracortical pyramidal cells, MDT-projecting neurons also display extensive dendritic arborizations into superficial PFC layers (Anastasiades et al., 2018), consistent with the large synaptic strength we observed in NAM-activated GFP(+) neurons. In addition, MDT-projecting neurons receive strong reciprocal projections from the MDT. Pharmacological potentiation of the MDT

inputs to the cortex, as with mGlu<sub>2</sub> or mGlu<sub>3</sub> NAM administration, would therefore be expected to preferentially activate type A neurons. Interestingly, a recent series of studies by Hare et al. (2019) demonstrated antidepressant-like efficacy following stimulation of D1-expressing neurons in the PFC. These neurons display the biophysical and anatomical properties present in “type B” cells and absent from type A cells (Anastasiades et al., 2019; Hare et al., 2019), suggesting that multiple PFC circuits govern affective behavioral responses. Based on this, investigating the cell type subpopulations that comprise antidepressant-activated ensembles is an interesting strategy to improve our understanding of how distinct PFC circuits regulate depressive-like behavior and anhedonia.

In addition to their output targets, differences in glutamatergic input could dictate which pyramidal cells are engaged during antidepressant treatments. For example, we recently discovered that PFC mGlu<sub>3</sub>-LTD is expressed at terminals originating from the BLA, but not the ventral hippocampus, and that mGlu<sub>2</sub> does not function at either synapse (Joffe et al.,

2019a). We would therefore predict that mGlu<sub>3</sub> NAM administration also recruits pyramidal cells that receive relatively greater input from the BLA. Future experiments that anatomically define PFC cell types *a priori* will shed light on these interesting and important questions. Furthermore, the PFC receives glutamatergic and monoaminergic inputs from a diverse set of cortices and nuclei within the basal forebrain and midbrain. How mGlu<sub>2</sub> and mGlu<sub>3</sub> shape neurotransmission at these synapses has not yet been explored and may be pertinent to fully understand the antidepressant-like efficacy of mGlu<sub>2</sub> and mGlu<sub>3</sub> NAMs.

The pronounced clinical and preclinical efficacy of ketamine has spurred a wave of research into the mechanism of action of rapid-acting antidepressants (Duman et al., 2016; Krystal et al., 2013; Zanos et al., 2018). The PFC is believed to be a key site of antidepressant action, where ketamine, scopolamine, and related molecules are thought to disinhibit pyramidal cells through the transient inhibition of GABAergic interneurons. The long-term antidepressant actions necessitate the initiation of protein translation, production of brain-derived neurotrophic factor (BDNF), and activation of its receptor tropomyosin-related kinase B (TrkB). In contrast to these mechanisms, we and others have shown that mGlu<sub>2</sub> and mGlu<sub>3</sub> receptors do not regulate monosynaptic inhibitory currents in the PFC (Joffe et al., 2019a; Kiritoshi and Neugebauer, 2015) and, moreover, that mGlu<sub>3</sub>-LTD of excitatory transmission does not occur on fast-spiking interneurons, suggesting that interneuron disinhibition is not essential for the efficacy of mGlu<sub>2</sub> and mGlu<sub>3</sub> NAMs. The antidepressant-like mechanisms of mGlu<sub>2</sub>/mGlu<sub>3</sub>-directed molecules therefore deviate from those of other rapid-acting treatments in several key ways. Instead, the present findings provide strong evidence that mGlu<sub>2</sub> and mGlu<sub>3</sub> NAMs directly enhance excitatory transmission onto PFC pyramidal cells. These effects are more proximal to the excitatory synapse than other novel antidepressant approaches and suggest that mGlu<sub>2</sub> and mGlu<sub>3</sub> NAMs may be preferable treatment options in clinical populations with suspected deficits in interneuron function, such as comorbid schizophrenia or schizoaffective disorder. Consistent with that notion, ketamine and scopolamine can produce psychotomimetic effects (Lahti et al., 2001; Lipowski, 1987), whereas no evidence suggests a similar risk for compounds that inhibit mGlu<sub>2</sub> or mGlu<sub>3</sub> and dual antagonists exhibit favorable profiles in preclinical models of ketamine-associated adverse effects (Witkin et al., 2017). Interestingly, the persistent efficacy of mGlu<sub>2/3</sub> antagonists has been shown to require BDNF (Koike et al., 2013) and mTOR signaling (Koike et al., 2011), suggesting overlap in the final common pathway between mGlu<sub>2</sub>/mGlu<sub>3</sub> NAMs, ketamine, and scopolamine. With that in mind, future studies should be directed at whether the long-term antidepressant actions of mGlu<sub>2</sub>/mGlu<sub>3</sub> NAMs also require protein translation, BDNF production, and TrkB receptor signaling. mGlu<sub>2</sub> and mGlu<sub>3</sub> also regulate neurotransmission at several synapses within the hippocampal circuit (Joffe et al., 2018), and these receptor populations merit study for their involvement in antidepressant-like behavioral responses.

On the other side of the coin, positive allosteric modulators (PAMs) for both mGlu<sub>2</sub> and mGlu<sub>3</sub> are being considered as

potential treatment approaches for schizophrenia and drug- and alcohol-use disorders (Joffe et al., 2018; Nicoletti et al., 2019). Preclinical studies have suggested that mGlu<sub>2</sub> activation exerts antipsychotic-like effects, whereas mGlu<sub>3</sub> may preferentially regulate cognition (Fujioka et al., 2014; Woolley et al., 2008). The data presented here are consistent with this analysis: mGlu<sub>2</sub> is positioned to attenuate excessive, psychosis-like MDT-PFC glutamate release (Marek et al., 2001; Moghaddam and Adams, 1998), whereas mGlu<sub>3</sub> gates the integration of postsynaptic information, an essential process for optimal working memory performance (Arnsten, 2015; Jin et al., 2018). This mechanistic divergence could potentially be exploited to design tailored approaches to treat coincident symptom clusters and/or comorbid diseases. For example, a patient with MDD and low cognitive function could be prescribed an mGlu<sub>2</sub> NAM to preserve the pro-cognitive function of endogenous mGlu<sub>3</sub>. Similarly, a patient with schizoaffective disorder could be treated with an mGlu<sub>3</sub> NAM for depressive-like symptoms, leaving intact the antipsychotic-like actions of endogenous mGlu<sub>2</sub>. Along these lines, a better understanding of how mGlu<sub>2</sub> and mGlu<sub>3</sub> each individually contribute to drug and alcohol seeking will be important for treating individuals with MDD and a comorbid substance abuse diagnosis. Although a previous trial for a non-selective mGlu<sub>2/3</sub> NAM did not display improvement relative to placebo (Wilkinson and Sanacora, 2019), the present findings have revealed that mGlu<sub>2</sub> and mGlu<sub>3</sub> recruit distinct mechanisms to modulate PFC function and related behaviors. These latent differences may be critical for achieving efficacy in separable clinical populations and should comprise an important consideration for future clinical trial design. Continued development and scrutiny of selective means to modulate mGlu<sub>2</sub> and mGlu<sub>3</sub> therefore provides opportunities to develop novel, personalized approaches to mitigate depressive symptomatology in MDD and other stress-related psychiatric disorders.

## STAR★METHODS

Detailed methods are provided in the online version of this paper and include the following:

- KEY RESOURCES TABLE
- LEAD CONTACT AND MATERIALS AVAILABILITY
- EXPERIMENTAL MODEL AND SUBJECT DETAILS
- METHOD DETAILS
  - In vivo drug administration
  - Stereotaxic injections
  - PFC slice preparation
  - Immunohistochemistry
  - Whole-cell electrophysiology
  - Locomotor activity
  - Tail suspension test
  - Forced swim test
  - Chronic CORT
  - Chronic variable stress (CVS)
  - Sucrose preference test
- QUANTIFICATION AND STATISTICAL ANALYSIS
- DATA AND CODE AVAILABILITY

## SUPPLEMENTAL INFORMATION

Supplemental Information can be found online at <https://doi.org/10.1016/j.neuron.2019.09.044>.

## ACKNOWLEDGMENTS

The authors thank Jennifer Zachry and Weimin Peng for technical assistance and other members of the Conn and Winder labs for stimulating discussions. This work was supported by NIH grants R01MH062646 and R37NS031373 (P.J.C.). M.E.J. was supported by NIH grant T32MH093366 and a postdoctoral fellowship through the Pharmaceutical Research and Manufacturers of America Foundation. C.I.S. was supported by the Searle Undergraduate Research Program. Some experiments were performed through the Murine Neurobehavior Core and Cell Imaging Shared Resource at Vanderbilt University Medical Center.

## AUTHOR CONTRIBUTIONS

Conceptualization, M.E.J. and P.J.C.; Investigation, M.E.J., C.I.S., K.H.O., and J.M.; Resources, N.A.H., J.L.E., C.W.L., and D.G.W.; Writing – Original Draft, M.E.J.; Writing – Review & Editing, all authors; Funding Acquisition, M.E.J. and P.J.C.

## DECLARATION OF INTERESTS

P.J.C. and C.W.L. receive research support from Lundbeck Pharmaceuticals and Boehringer Ingelheim, and C.W.L. also receives support from Ono Pharmaceutical. P.J.C. and C.W.L. are inventors on multiple patents for allosteric modulators for several classes of metabotropic glutamate receptors. M.E.J., C.I.S., K.H.O., J.M., N.A.H., J.L.E., and D.G.W. declare no competing interests.

Received: April 16, 2019

Revised: August 14, 2019

Accepted: September 25, 2019

Published: November 14, 2019

## REFERENCES

- An, J., Wang, L., Li, K., Zeng, Y., Su, Y., Jin, Z., Yu, X., and Si, T. (2017). Differential effects of antidepressant treatment on long-range and short-range functional connectivity strength in patients with major depressive disorder. *Sci. Rep.* *7*, 10214.
- Anastasiades, P.G., Marlin, J.J., and Carter, A.G. (2018). Cell-type specificity of callosally evoked excitation and feedforward inhibition in the prefrontal cortex. *Cell Rep.* *22*, 679–692.
- Anastasiades, P.G., Boada, C., and Carter, A.G. (2019). Cell-type-specific D1 dopamine receptor modulation of projection neurons and interneurons in the prefrontal cortex. *Cereb. Cortex* *29*, 3224–3242.
- Arnsten, A.F. (2015). Stress weakens prefrontal networks: molecular insults to higher cognition. *Nat. Neurosci.* *18*, 1376–1385.
- Barth, A.L., Gerkin, R.C., and Dean, K.L. (2004). Alteration of neuronal firing properties after in vivo experience in a FosGFP transgenic mouse. *J. Neurosci.* *24*, 6466–6475.
- Bocchio, M., Lukacs, I.P., Stacey, R., Plaha, P., Apostolopoulos, V., Livermore, L., Sen, A., Anson, O., Gillies, M.J., Somogyi, P., and Capogna, M. (2019). Group II metabotropic glutamate receptors mediate presynaptic inhibition of excitatory transmission in pyramidal neurons of the human cerebral cortex. *Front. Cell. Neurosci.* *12*, 508.
- Bollinger, K.A., Felts, A.S., Brassard, C.J., Engers, J.L., Rodriguez, A.L., Weiner, R.L., Cho, H.P., Chang, S., Bubser, M., Jones, C.K., et al. (2017). Design and synthesis of mGlu<sub>2</sub> NAMs with improved potency and CNS penetration based on a truncated picolinamide core. *ACS Med. Chem. Lett.* *8*, 919–924.
- Caetano, S.C., Kaur, S., Brambilla, P., Nicoletti, M., Hatch, J.P., Sassi, R.B., Mallinger, A.G., Keshavan, M.S., Kupfer, D.J., Frank, E., and Soares, J.C. (2006). Smaller cingulate volumes in unipolar depressed patients. *Biol. Psychiatry* *59*, 702–706.
- Chaki, S. (2017). mGlu<sub>2/3</sub> receptor antagonists as novel antidepressants. *Trends Pharmacol. Sci.* *38*, 569–580.
- Chaki, S., Yoshikawa, R., Hirota, S., Shimazaki, T., Maeda, M., Kawashima, N., Yoshimizu, T., Yasuhara, A., Sakagami, K., Okuyama, S., et al. (2004). MGS0039: a potent and selective group II metabotropic glutamate receptor antagonist with antidepressant-like activity. *Neuropharmacology* *46*, 457–467.
- Collins, D.P., Anastasiades, P.G., Marlin, J.J., and Carter, A.G. (2018). Reciprocal circuits linking the prefrontal cortex with dorsal and ventral thalamic nuclei. *Neuron* *98*, 366–379.e4.
- Cryan, J.F., Mombereau, C., and Vassout, A. (2005). The tail suspension test as a model for assessing antidepressant activity: review of pharmacological and genetic studies in mice. *Neurosci. Biobehav. Rev.* *29*, 571–625.
- Delevich, K., Tucciarone, J., Huang, Z.J., and Li, B. (2015). The mediodorsal thalamus drives feedforward inhibition in the anterior cingulate cortex via parvalbumin interneurons. *J. Neurosci.* *35*, 5743–5753.
- Di Menna, L., Joffe, M.E., Iacovelli, L., Orlando, R., Lindsley, C.W., Mairesse, J., Gressens, P., Cannella, M., Caraci, F., Copani, A., et al. (2018). Functional partnership between mGlu<sub>3</sub> and mGlu<sub>5</sub> metabotropic glutamate receptors in the central nervous system. *Neuropharmacology* *128*, 301–313.
- Dong, C., Zhang, J.C., Yao, W., Ren, Q., Ma, M., Yang, C., Chaki, S., and Hashimoto, K. (2017). Rapid and sustained antidepressant action of the mGlu<sub>2/3</sub> receptor antagonist MGS0039 in the social defeat stress model: comparison with ketamine. *Int. J. Neuropsychopharmacol.* *20*, 228–236.
- Duman, R.S., Aghajanian, G.K., Sanacora, G., and Krystal, J.H. (2016). Synaptic plasticity and depression: new insights from stress and rapid-acting antidepressants. *Nat. Med.* *22*, 238–249.
- Dwyer, J.M., Lepack, A.E., and Duman, R.S. (2013). mGluR<sub>2/3</sub> blockade produces rapid and long-lasting reversal of anhedonia caused by chronic stress exposure. *J. Mol. Psychiatry* *1*, 15.
- Engers, J.L., Rodriguez, A.L., Konkol, L.C., Morrison, R.D., Thompson, A.D., Byers, F.W., Blobaum, A.L., Chang, S., Venable, D.F., Loch, M.T., et al. (2015). Discovery of a selective and CNS penetrant negative allosteric modulator of metabotropic glutamate receptor subtype 3 with antidepressant and anxiolytic activity in rodents. *J. Med. Chem.* *58*, 7485–7500.
- Engers, J.L., Bollinger, K.A., Weiner, R.L., Rodriguez, A.L., Long, M.F., Breiner, M.M., Chang, S., Bollinger, S.R., Bubser, M., Jones, C.K., et al. (2017). Design and synthesis of *N*-aryl phenoxyethoxy pyridinones as highly selective and CNS penetrant mGlu<sub>3</sub> NAMs. *ACS Med. Chem. Lett.* *8*, 925–930.
- Fenno, L.E., Mattis, J., Ramakrishnan, C., Hyun, M., Lee, S.Y., He, M., Tucciarone, J., Selimbeyoglu, A., Berndt, A., Grosenick, L., et al. (2014). Targeting cells with single vectors using multiple-feature Boolean logic. *Nat. Methods* *11*, 763–772.
- Fujioka, R., Nii, T., Iwaki, A., Shibata, A., Ito, I., Kitaichi, K., Nomura, M., Hattori, S., Takao, K., Miyakawa, T., and Fukumaki, Y. (2014). Comprehensive behavioral study of mGluR3 knockout mice: implication in schizophrenia related endophenotypes. *Mol. Brain* *7*, 31.
- Fukumoto, K., Iijima, M., and Chaki, S. (2016). The antidepressant effects of an mGlu<sub>2/3</sub> receptor antagonist and ketamine require AMPA receptor stimulation in the mPFC and subsequent activation of the 5-HT neurons in the DRN. *Neuropsychopharmacology* *41*, 1046–1056.
- Gaynes, B.N., Warden, D., Trivedi, M.H., Wisniewski, S.R., Fava, M., and Rush, A.J. (2009). What did STAR\*D teach us? Results from a large-scale, practical, clinical trial for patients with depression. *Psychiatr. Serv.* *60*, 1439–1445.
- Gould, T.D., Zarate, C.A., Jr., and Thompson, S.M. (2019). Molecular pharmacology and neurobiology of rapid-acting antidepressants. *Annu. Rev. Pharmacol. Toxicol.* *59*, 213–236.
- Gourley, S.L., and Taylor, J.R. (2009). Recapitulation and reversal of a persistent depression-like syndrome in rodents. *Curr. Protoc. Neurosci. Chapter 9*. Unit 9.32.
- Gourley, S.L., Kiraly, D.D., Howell, J.L., Olausson, P., and Taylor, J.R. (2008a). Acute hippocampal brain-derived neurotrophic factor restores motivational

- and forced swim performance after corticosterone. *Biol. Psychiatry* *64*, 884–890.
- Gourley, S.L., Wu, F.J., Kiraly, D.D., Ploski, J.E., Kedves, A.T., Duman, R.S., and Taylor, J.R. (2008b). Regionally specific regulation of ERK MAP kinase in a model of antidepressant-sensitive chronic depression. *Biol. Psychiatry* *63*, 353–359.
- Hare, B.D., Shinohara, R., Liu, R.J., Pothula, S., DiLeone, R.J., and Duman, R.S. (2019). Optogenetic stimulation of medial prefrontal cortex Drd1 neurons produces rapid and long-lasting antidepressant effects. *Nat. Commun.* *10*, 223.
- Harris, N.A., Isaac, A.T., Günther, A., Merkel, K., Melchior, J., Xu, M., Eguakun, E., Perez, R., Nabit, B.P., Flavin, S., et al. (2018). Dorsal BNST  $\alpha_{2A}$ -adrenergic receptors produce HCN-dependent excitatory actions that initiate anxiogenic behaviors. *J. Neurosci.* *38*, 8922–8942.
- Hasler, G., van der Veen, J.W., Tuminis, T., Meyers, N., Shen, J., and Drevets, W.C. (2007). Reduced prefrontal glutamate/glutamine and gamma-aminobutyric acid levels in major depression determined using proton magnetic resonance spectroscopy. *Arch. Gen. Psychiatry* *64*, 193–200.
- Hetzener, A., Corti, C., Herdy, S., Corsi, M., Ferraguti, F., and Singewald, N. (2008). Individual contribution of metabotropic glutamate receptor (mGlu) 2 and 3 to c-Fos expression pattern evoked by mGlu2/3 antagonism. *Psychopharmacology (Berl.)* *201*, 1–13.
- Highland, J.N., Zanos, P., Georgiou, P., and Gould, T.D. (2019). Group II metabotropic glutamate receptor blockade promotes stress resilience in mice. *Neuropsychopharmacology* *44*, 1788–1796.
- Jin, L.E., Wang, M., Galvin, V.C., Lightbourne, T.C., Conn, P.J., Arnsten, A.F.T., and Paspalas, C.D. (2018). mGluR2 versus mGluR3 metabotropic glutamate receptors in primate dorsolateral prefrontal cortex: postsynaptic mGluR3 strengthen working memory networks. *Cereb. Cortex* *28*, 974–987.
- Joffe, M.E., and Conn, P.J. (2019). Antidepressant potential of metabotropic glutamate receptor mGlu<sub>2</sub> and mGlu<sub>3</sub> negative allosteric modulators. *Neuropsychopharmacology* *44*, 214–236.
- Joffe, M.E., and Grueter, B.A. (2016). Cocaine experience enhances thalamo-accumbens N-methyl-D-aspartate receptor function. *Biol. Psychiatry* *80*, 671–681.
- Joffe, M.E., Vitter, S.R., and Grueter, B.A. (2017). GluN1 deletions in D1- and A2A-expressing cell types reveal distinct modes of behavioral regulation. *Neuropharmacology* *112* (Pt A), 172–180.
- Joffe, M.E., Centanni, S.W., Jaramillo, A.A., Winder, D.G., and Conn, P.J. (2018). Metabotropic glutamate receptors in alcohol use disorder: physiology, plasticity, and promising pharmacotherapies. *ACS Chem. Neurosci.* *9*, 2188–2204.
- Joffe, M.E., Santiago, C.I., Engers, J.L., Lindsley, C.W., and Conn, P.J. (2019a). Metabotropic glutamate receptor subtype 3 gates acute stress-induced dysregulation of amygdalo-cortical function. *Mol. Psychiatry* *24*, 916–927.
- Joffe, M.E., Santiago, C.I., Stansley, B.J., Maksymetz, J., Gogliotti, R.G., Engers, J.L., Nicoletti, F., Lindsley, C.W., and Conn, P.J. (2019b). Mechanisms underlying prelimbic prefrontal cortex mGlu<sub>3</sub>/mGlu<sub>5</sub>-dependent plasticity and reversal learning deficits following acute stress. *Neuropharmacology* *144*, 19–28.
- Johnson, K.A., Mateo, Y., and Lovinger, D.M. (2017). Metabotropic glutamate receptor 2 inhibits thalamically-driven glutamate and dopamine release in the dorsal striatum. *Neuropharmacology* *117*, 114–123.
- Kang, H.J., Voleti, B., Hajszan, T., Rajkowska, G., Stockmeier, C.A., Licznarski, P., Lepack, A., Majik, M.S., Jeong, L.S., Banasr, M., et al. (2012). Decreased expression of synapse-related genes and loss of synapses in major depressive disorder. *Nat. Med.* *18*, 1413–1417.
- Kavalali, E.T., and Monteggia, L.M. (2012). Synaptic mechanisms underlying rapid antidepressant action of ketamine. *Am. J. Psychiatry* *169*, 1150–1156.
- Kiritoshi, T., and Neugebauer, V. (2015). Group II mGluRs modulate baseline and arthritis pain-related synaptic transmission in the rat medial prefrontal cortex. *Neuropharmacology* *95*, 388–394.
- Koike, H., Iijima, M., and Chaki, S. (2011). Involvement of the mammalian target of rapamycin signaling in the antidepressant-like effect of group II metabotropic glutamate receptor antagonists. *Neuropharmacology* *61*, 1419–1423.
- Koike, H., Fukumoto, K., Iijima, M., and Chaki, S. (2013). Role of BDNF/TrkB signaling in antidepressant-like effects of a group II metabotropic glutamate receptor antagonist in animal models of depression. *Behav. Brain Res.* *238*, 48–52.
- Krystal, J.H., Sanacora, G., and Duman, R.S. (2013). Rapid-acting glutamatergic antidepressants: the path to ketamine and beyond. *Biol. Psychiatry* *73*, 1133–1141.
- Kupferschmidt, D.A., Cody, P.A., Lovinger, D.M., and Davis, M.I. (2015). Brain BLAQ: Post-hoc thick-section histochemistry for localizing optogenetic constructs in neurons and their distal terminals. *Front. Neuroanat.* *9*, 6.
- Lahti, A.C., Weiler, M.A., Tamara Michaelidis, B.A., Parwani, A., and Tamminga, C.A. (2001). Effects of ketamine in normal and schizophrenic volunteers. *Neuropsychopharmacology* *25*, 455–467.
- Linden, A.M., Bergeron, M., and Schoepp, D.D. (2005). Comparison of c-Fos induction in the brain by the mGlu2/3 receptor antagonist LY341495 and agonist LY354740: evidence for widespread endogenous tone at brain mGlu2/3 receptors in vivo. *Neuropharmacology* *49* (Suppl 1), 120–134.
- Linden, A.M., Johnson, B.G., Trokovic, N., Korpi, E.R., and Schoepp, D.D. (2009). Use of MGLUR2 and MGLUR3 knockout mice to explore in vivo receptor specificity of the MGLUR2/3 selective antagonist LY341495. *Neuropharmacology* *57*, 172–182.
- Lipowski, Z.J. (1987). Delirium (acute confusional states). *JAMA* *258*, 1789–1792.
- Lourenço Neto, F., Schadrack, J., Berthele, A., Zieglgänsberger, W., Tölle, T.R., and Castro-Lopes, J.M. (2000). Differential distribution of metabotropic glutamate receptor subtype mRNAs in the thalamus of the rat. *Brain Res.* *854*, 93–105.
- Marek, G.J., Wright, R.A., Schoepp, D.D., Monn, J.A., and Aghajanian, G.K. (2000). Physiological antagonism between 5-hydroxytryptamine(2A) and group II metabotropic glutamate receptors in prefrontal cortex. *J. Pharmacol. Exp. Ther.* *292*, 76–87.
- Marek, G.J., Wright, R.A., Gewirtz, J.C., and Schoepp, D.D. (2001). A major role for thalamocortical afferents in serotonergic hallucinogen receptor function in the rat neocortex. *Neuroscience* *105*, 379–392.
- Miller, O.H., Bruns, A., Ben Ammar, I., Mueggler, T., and Hall, B.J. (2017). Synaptic regulation of a thalamocortical circuit controls depression-related behavior. *Cell Rep.* *20*, 1867–1880.
- Moghaddam, B., and Adams, B.W. (1998). Reversal of phencyclidine effects by a group II metabotropic glutamate receptor agonist in rats. *Science* *281*, 1349–1352.
- Morishima, Y., Miyakawa, T., Furuyashiki, T., Tanaka, Y., Mizuma, H., and Nakanishi, S. (2005). Enhanced cocaine responsiveness and impaired motor coordination in metabotropic glutamate receptor subtype 2 knockout mice. *Proc. Natl. Acad. Sci. USA* *102*, 4170–4175.
- Nicoletti, F., Orlando, R., Di Menna, L., Cannella, M., Notartomaso, S., Mascio, G., Iacovelli, L., Matriciano, F., Fazio, F., Caraci, F., et al. (2019). Targeting mGlu receptors for optimization of antipsychotic activity and disease-modifying effect in schizophrenia. *Front. Psychiatry* *10*, 49.
- Ohishi, H., Shigemoto, R., Nakanishi, S., and Mizuno, N. (1993a). Distribution of the messenger RNA for a metabotropic glutamate receptor, mGluR2, in the central nervous system of the rat. *Neuroscience* *53*, 1009–1018.
- Ohishi, H., Shigemoto, R., Nakanishi, S., and Mizuno, N. (1993b). Distribution of the mRNA for a metabotropic glutamate receptor (mGluR3) in the rat brain: an in situ hybridization study. *J. Comp. Neurol.* *335*, 252–266.
- Rajkowska, G. (2000). Postmortem studies in mood disorders indicate altered numbers of neurons and glial cells. *Biol. Psychiatry* *48*, 766–777.
- Siegle, G.J., Thompson, W., Carter, C.S., Steinhauer, S.R., and Thase, M.E. (2007). Increased amygdala and decreased dorsolateral prefrontal BOLD responses in unipolar depression: related and independent features. *Biol. Psychiatry* *61*, 198–209.

- Solich, J., Palach, P., Budziszewska, B., and Dziedzicka-Wasylewska, M. (2008). Effect of two behavioral tests on corticosterone level in plasma of mice lacking the noradrenaline transporter. *Pharmacol. Rep.* *60*, 1008–1013.
- Sturm, M., Becker, A., Schroeder, A., Bilkei-Gorzo, A., and Zimmer, A. (2015). Effect of chronic corticosterone application on depression-like behavior in C57BL/6N and C57BL/6J mice. *Genes Brain Behav.* *14*, 292–300.
- Thuault, S.J., Malleret, G., Constantinople, C.M., Nicholls, R., Chen, I., Zhu, J., Panteleyev, A., Vronskaya, S., Nolan, M.F., Bruno, R., et al. (2013). Prefrontal cortex HCN1 channels enable intrinsic persistent neural firing and executive memory function. *J. Neurosci.* *33*, 13583–13599.
- Vardy, E., Robinson, J.E., Li, C., Olsen, R.H.J., DiBerto, J.F., Giguere, P.M., Sassano, F.M., Huang, X.P., Zhu, H., Urban, D.J., et al. (2015). A new DREADD facilitates the multiplexed chemogenetic interrogation of behavior. *Neuron* *86*, 936–946.
- Walker, A.G., Wenthur, C.J., Xiang, Z., Rook, J.M., Emmitte, K.A., Niswender, C.M., Lindsley, C.W., and Conn, P.J. (2015). Metabotropic glutamate receptor 3 activation is required for long-term depression in medial prefrontal cortex and fear extinction. *Proc. Natl. Acad. Sci. USA* *112*, 1196–1201.
- Walter, M., Henning, A., Grimm, S., Schulte, R.F., Beck, J., Dydak, U., Schnepf, B., Boeker, H., Boesiger, P., and Northoff, G. (2009). The relationship between aberrant neuronal activation in the pregenual anterior cingulate, altered glutamatergic metabolism, and anhedonia in major depression. *Arch. Gen. Psychiatry* *66*, 478–486.
- Wellman, C.L. (2001). Dendritic reorganization in pyramidal neurons in medial prefrontal cortex after chronic corticosterone administration. *J. Neurobiol.* *49*, 245–253.
- Wilkinson, S.T., and Sanacora, G. (2019). A new generation of antidepressants: an update on the pharmaceutical pipeline for novel and rapid-acting therapeutics in mood disorders based on glutamate/GABA neurotransmitter systems. *Drug Discov. Today* *24*, 606–615.
- Willner, P. (2016). Reliability of the chronic mild stress model of depression: a user survey. *Neurobiol. Stress* *6*, 68–77.
- Witkin, J.M., Monn, J.A., Li, J., Johnson, B., McKinzie, D.L., Wang, X.S., Heinz, B.A., Li, R., Ornstein, P.L., Smith, S.C., et al. (2017). Preclinical predictors that the orthosteric mGlu2/3 receptor antagonist LY3020371 will not engender ketamine-associated neurotoxic, motor, cognitive, subjective, or abuse-liability-related effects. *Pharmacol. Biochem. Behav.* *155*, 43–55.
- Woolley, M.L., Pemberton, D.J., Bate, S., Corti, C., and Jones, D.N. (2008). The mGlu2 but not the mGlu3 receptor mediates the actions of the mGluR2/3 agonist, LY379268, in mouse models predictive of antipsychotic activity. *Psychopharmacology (Berl.)* *196*, 431–440.
- Yuen, E.Y., Wei, J., Liu, W., Zhong, P., Li, X., and Yan, Z. (2012). Repeated stress causes cognitive impairment by suppressing glutamate receptor expression and function in prefrontal cortex. *Neuron* *73*, 962–977.
- Zanos, P., and Gould, T.D. (2018). Mechanisms of ketamine action as an antidepressant. *Mol. Psychiatry* *23*, 801–811.
- Zanos, P., Moaddel, R., Morris, P.J., Riggs, L.M., Highland, J.N., Georgiou, P., Pereira, E.F.R., Albuquerque, E.X., Thomas, C.J., Zarate, C.A., Jr., and Gould, T.D. (2018). Ketamine and ketamine metabolite pharmacology: insights into therapeutic mechanisms. *Pharmacol. Rev.* *70*, 621–660.
- Zanos, P., Highland, J.N., Stewart, B.W., Georgiou, P., Jenne, C.E., Lovett, J., Morris, P.J., Thomas, C.J., Moaddel, R., Zarate, C.A., Jr., and Gould, T.D. (2019). (2*R*,6*R*)-hydroxynorketamine exerts mGlu<sub>2</sub> receptor-dependent antidepressant actions. *Proc. Natl. Acad. Sci. USA* *116*, 6441–6450.

## STAR★METHODS

### KEY RESOURCES TABLE

Reagent or Resource	Source	Identifier
<b>Antibodies</b>		
primary Chicken anti-GFP, 1:1000	Abcam	ab13970; RRID:AB_300798
secondary Goat anti-Chicken, 488 nm 1:500	Invitrogen	A-11039; RRID:AB_2534096
Hoescht 33342, 1:1000	Thermo Fisher Scientific	H3570
<b>Bacterial and Virus Strains</b>		
AAV5-CaMKII-ChR2-EYFP	UNC Vector Core	N/A
rgAAV-Ef1a-mCherry-IRES-Cre	<a href="#">Fenno et al., 2014</a>	Cat # 65417-AAV8
AAV8-hSyn-dF-HA-KORD-IRES-mCitrine	<a href="#">Vardy et al., 2015</a>	Cat # 55632-AAVrg
<b>Chemicals, Peptides, and Recombinant Proteins</b>		
LY341495	Tocris	Cat # 1209
LY379268	Tocris	Cat # 5064
LY395756	Tocris	Cat # 3272
MRK-829	CW Lindsley; <a href="#">Walker et al., 2015</a>	N/A
VU6001966	CW Lindsley; <a href="#">Bollinger et al., 2017</a>	N/A
VU0650786	CW Lindsley; <a href="#">Engers et al., 2015</a>	N/A
Salvinorin B	HelloBio	Cat # HB4887
<b>Experimental Models: Organisms/Strains</b>		
Mouse: C57BL/6J	The Jackson Laboratory	RRID: IMSR_JAX:000664
Mouse: cfos-EGFP	The Jackson Laboratory	RRID: IMSR_JAX:014135
<b>Software and Algorithms</b>		
pClamp	Molecular Devices	RRID: SCR_011323
Prism 8.0	GraphPad Software	RRID: SCR_002798

### LEAD CONTACT AND MATERIALS AVAILABILITY

New reagents were not developed during these studies. Further information and requests for resources and reagents should be directed to and will be fulfilled by the Lead Contact, P. Jeffrey Conn ([jeff.conn@vanderbilt.edu](mailto:jeff.conn@vanderbilt.edu)).

### EXPERIMENTAL MODEL AND SUBJECT DETAILS

Adult (8-12-week-old) C57BL/6J male mice (Jackson Laboratories, Stock No: 000664) were group housed in a controlled environment (lights on at 6:00am) with food and water available *ad libitum*. Transgenic *cfos-EGFP* mice (Jackson Laboratories, Stock No: 014135) were bred in-house as described ([Barth et al., 2004](#); [Harris et al., 2018](#)). All procedures were performed in accordance with Vanderbilt University Animal Care and Use Committee and guidelines set forth by the *Guide for the Care and Use of Laboratory Animals*.

### METHOD DETAILS

#### In vivo drug administration

VU6001966 and VU0650786 were administered via intraperitoneal (*i.p.*) injections (10  $\mu$ L/g 10% v/v Tween 80 vehicle) 45 minutes prior to sacrifice for electrophysiology, the tail suspension test, and the forced swim test; and 24 hours prior to the sucrose preference test. After NAM administration, mice were isolated in a disposable cardboard bucket or remained in their home cages for electrophysiology and behavioral experiments, respectively. Mice were habituated to injections for 2-3 days prior to experimentation. Doses were selected based on published pharmacokinetic analyses to achieve unbound brain concentrations approximately 3-fold higher than each NAM's  $IC_{50}$  ([Bollinger et al., 2017](#); [Engers et al., 2015](#)). Salvinorin B (SALB) was administered via subcutaneous (*s.c.*) injection (1  $\mu$ L/g 100% DMSO vehicle) 10 minutes prior to behavioral experiments. LY379268, LY341495, and LY395756 were purchased from Tocris. SALB was purchased from HelloBio. VU6001966, VU0650786, and MRK-8-29 were synthesized in-house.

### Stereotaxic injections

Channelrhodopsin-2 (ChR2) or the  $\kappa$  opioid receptor DREADD (KORD) were virally expressed in glutamatergic neurons as described (Joffe and Grueter, 2016). Mice were anesthetized with isoflurane and 300–400 nL virus (AAV5-CaMKII-ChR2-EYFP, University of North Carolina; AAV8-hSyn-dF-KORD-mCitrine, Addgene) was delivered to the MDT (ML:  $\pm$  0.4 mm, AP:  $-1.5$ , DV:  $-3.5$ ). For KORD studies, 400 nL retrograde virus expressing Cre recombinase (AAVrg-Ef1a-mCherry-IRES-Cre, Addgene) was also delivered to the PFC (ML:  $\pm$  0.4 mm, AP: 1.9, DV:  $-2.0$ ). pAAV-hSyn-dF-HA-KORD-IRES-mCitrine was a gift from Bryan Roth (Addgene viral prep # 65417-AAV8) (Vardy et al., 2015). pAAV-Ef1a-mCherry-IRES-Cre was a gift from Karl Deisseroth (Addgene viral prep # 55632-AAVrg) (Fenno et al., 2014). Mice received carprofen for 72 hours following the procedure.

### PFC slice preparation

Slices and recordings were made as described (Di Menna et al., 2018). Briefly, mice were anesthetized with isoflurane and decapitated. Coronal slices (300  $\mu$ M) were prepared using an *N*-methyl-D-glucamine-based cutting and recovery solution. The artificial cerebrospinal fluid (aCSF) solute concentrations were (in mM): 119 NaCl, 2.5 KCl, 2.5 CaCl<sub>2</sub>, 1.3 MgCl<sub>2</sub>, 1 NaH<sub>2</sub>PO<sub>4</sub>, 11 glucose, and 26 NaHCO<sub>3</sub>. For the c-Fos immunohistochemistry and electrophysiology studies, slices were prepared from the same mice but used for only one experiment.

### Immunohistochemistry

For c-Fos induction studies, slices recovered in aCSF for 1 hour and were then fixed using 4% PFA for 1–2 hours and transferred to PBS. Fixed slices underwent BLAQ processing (Kupferschmidt et al., 2015) prior to incubation with Hoescht nuclear stain and antibodies to detect GFP (Chicken anti-GFP, Abcam, 1:1000; Goat anti-Chicken 488, Invitrogen, 1:500). Images at 20X (0.50 Plan Neofluar) were taken within layer 5 of the prelimbic PFC with a light confocal microscope (LSM 710 META Inverted). Image processing was performed using Fiji-ImageJ. Cell counts were calculated by adjusting the threshold automatically with Li setting. All particles fitting within the range of 20–100  $\mu$ m and a 0–1.0 circularity for the Hoechst staining were counted as cells. c-Fos-positive cells were tabulated using the same setting on the GFP channel.

### Whole-cell electrophysiology

The recording chamber was perfused with warm ( $30 \pm 1^\circ\text{C}$ ), oxygenated (95% O<sub>2</sub> / 5% CO<sub>2</sub>) aCSF at 2 ml/min. Prelimbic PFC pyramidal cells in layer 5 were filled with a K-based solution (in mM): 125 K-gluconate, 4 NaCl, 10 HEPES, 4 MgATP, 0.3 NaGTP, 10 Tris-phosphocreatine. Passive and active membrane properties were collected in current-clamp configuration. A series of 20, 1 s current injections were applied, beginning at  $-150$  pA, incremented at 25 pA, and culminating at  $+200$  pA.  $R_m$  was calculated as the slope of the hyperpolarized potentials divided by the current injected. Sag ratio was calculated after a  $-150$  pA injection by dividing the difference between the peak and steady-state hyperpolarization by the steady-state hyperpolarization. Post hoc Bonferonni comparisons were used to assess differences between GFP(+) and GFP(-) pyramidal cells within each treatment group. Optogenetic excitatory postsynaptic currents (op-EPSCs) were elicited with 1–3 ms 470 nm light stimulation. LTD was induced by applying 200 nM LY379268 for 10 minutes (Di Menna et al., 2018; Joffe et al., 2019a, 2019b). NAMs were bath-applied in 0.1% DMSO for at least 30 mins prior to LY379268 wash-on or PPR assessment. SALB was applied at 200 nM in 5% DMSO for 20 minutes. All drug concentrations were selected to be 30-fold higher than its EC<sub>50</sub>/IC<sub>50</sub>. No more than 4 neurons per cell type were collected from any individual animal.

### Locomotor activity

Mice were placed in an open field chamber where their movement was tracked with horizontal infrared beams and specialized software (MedAssociates, VT). Several locomotor measurements, including horizontal locomotion, stationary time, vertical counts, and stereotypic counts, were gathered over the course of a 2-hour test. After 1 hour, they were removed from the chamber, administered vehicle or NAMs, and immediately returned to the chamber for the remainder of the session. For the KORD study, mice received DMSO or SALB 10 minutes prior to the 1 hour test, without any prior habituation to the apparatus.

### Tail suspension test

The tail suspension test was performed as described (Engers et al., 2017). Mice were suspended by their tails from a force transducer for 6 minutes and immobility was tracked with automated software (MedAssociates, VT). Total time of immobility and latency to the first 10 s immobile bout were recorded.

### Forced swim test

The forced swim test was performed as described (Joffe et al., 2017). Swim sessions were conducted once for 6 minutes and were manually scored by a blinded observer. Total time of immobility and latency to the first 10 s immobile bout were recorded.

### Chronic CORT

CORT was administered via home cage drinking water (Gourley et al., 2008a; Gourley and Taylor, 2009). Beta-cyclodextrin ( $\beta$ -CD) vehicle (final concentration 0.5% w/v) was used to enhance CORT solubility. Mice were treated for 3 weeks with 80  $\mu$ g/ml CORT

(approximately 20–22 mg/kg/day; [Gourley et al., 2008a](#)), then tapered for 3 days at 40  $\mu$ g/ml and 3 days at 20  $\mu$ g/ml. Normal drinking water was returned for a 1-week CORT-free washout prior to experimentation.

### **Chronic variable stress (CVS)**

CVS was administered for 4 weeks and subsequent behavioral testing commenced after 1 week without stress. Stressors were selected based on results of a recent survey ([Willner, 2016](#)), and consisted of restraint (2–4 hr), cage tilt (45°, 4–10 hr), foot shock (2  $\times$  0.3 mA, 1 s), soiled cage (250 mL water, 4–18 hr), novel object (4–18 hr), and empty cage (4–18 hr). Stressors were presented in a pseudo-random order, once or twice per day, for 6 days each week. The soiled cage, novel object, and empty cage stressors were often conducted overnight. The presentation was varied such that the same stress was not applied twice within 3 consecutive days. Soiled and empty cage stressors concluded by transferring mice to a new cage.

### **Sucrose preference test**

Mice were habituated to 2-bottle cages 2 days prior to testing and given free access to sucrose (2% w/v) for 2 hours. The following day, access to food and water was restricted for 4 hours prior to testing. Individualized testing occurred in new cages with one bottle containing sucrose and the other containing normal drinking water. Cages were placed in an isolated cabinet for 6 hours and mice were returned to group housing after completion of the test. To calculate the amount consumed, all bottles were weighed before and after testing and corrected for the average weight lost in control bottles.

### **QUANTIFICATION AND STATISTICAL ANALYSIS**

The number of cells or mice for each experiment is denoted by “n” or “N” respectively. Each behavioral experiment was replicated in at least 2 cohorts of mice. Data are presented as mean  $\pm$  standard error. Analyses were performed using GraphPad Prism. One-sample t test, two-tailed Student’s t test, and one-way or two-way ANOVA with Bonferroni post hoc comparisons were used as appropriate. Statistical results are displayed in the figure legends.

### **DATA AND CODE AVAILABILITY**

The datasets supporting the current study are available from the corresponding author on request.